How climate shapes the functioning of Tropical Montane Cloud Forests

Cleiton B Eller[1,2], Leonardo D Meireles[3], Stephen Sitch[1], Stephen SO Burgess[4], Rafael S Oliveira[2]

1- College of Life and Environmental Sciences, University of Exeter, Exeter, EX4 4QF, UK.

2- Departamento de Biologia Vegetal, Universidade de Campinas, Campinas, 13083-862, Brasil.

3- Universidade de São Paulo, Escola de Artes, Ciências e Humanidades, São Paulo, 03828-000, Brasil.

4- University of Western Australia, School of Plant Biology, Perth, WA 6009, Australia.

Corresponding author: Cleiton B Eller (c.breder-eller@exeter.ac.uk)

Abstract

Purpose of Review: Tropical Montane Cloud Forest (TMCF) is a highly vulnerable ecosystem which occurs at higher elevations in tropical mountains. Many aspects of TMCF vegetation functioning are poorly understood, making it difficult to quantify and project TMCF vulnerability to global change. We compile functional traits data to provide an overview of TMCF functional ecology. We use numerical models to understand the consequences of TMCF functional composition with respect to its responses to climate and link the traits of TMCF to its environmental conditions.

Recent Findings: TMCF leaves are small and have low SLA but high Rubisco content per leaf area. This implies that TMCF maximum net leaf carbon assimilation (A_n) is high, but often limited by low temperature and leaf wetting. Cloud immersion provides important water, and potentially nutrient, inputs to TMCF plants. TMCF species possess low sapwood specific conductivity which is compensated with a lower tree height and higher sapwood to leaf area ratio. These traits associated with a more conservative stomatal regulation results in a higher hydraulic safety margin than nearby forests not affected by clouds. The architecture of TMCF trees including its proportionally thicker trunks and large root systems increase tree mechanical stability.

Summary: The TMCF functional traits can be conceptually linked to its colder and cloudy environment limiting A_n, growth, water transport and nutrient availability. A hotter climate would drastically affect the abiotic filters shaping TMCF communities and potentially facilitate the invasion of TMCF by more productive lowland species.

Key words: Climate change, Cloud forests, Functional traits, Plant hydraulics, Photosynthesis

Acknowledgments: This research was supported by the Newton Fund through the Met Office Climate Science for Service Partnership Brazil (CSSP Brazil), the NERC grant NE/R00532X/1 and FAPESP grant 11/52072-0.

1. Introduction

Tropical Montane Cloud Forest (TMCF) is a rare ecosystem type which covers only 0.26% of Earth's land surface [1]. Despite its restricted distribution, TMCF hosts a large biodiversity [1–3•] and provides important ecosystem services in mountainous regions [1,3–5]. Cloud immersion events are the main climatic attribute defining TMCF [6,7]. The increase in the cloud immersion frequency at higher altitudes produces a progressively shorter vegetation with smaller leaves, and trunks and branches covered by epiphytes [4,7,8•]. This shift in vegetation structure is accompanied by changes in the floristic community composition [9–11•]. There is a marked drop in the abundance of Fabaceae [10,11•], while Myrtaceae and several Magnoliid families become more abundant [8,12–14].

TMCF exhibits an extremely high plant species richness per unit area [3]. For example, Mexican TMCF cover less than 1% of its territory but contain 650 genera of vascular plants with at least one species endemic or preferentially associated to TMCF [15]. While overall tree diversity tends to decline with altitude [2], pteridophytes and epiphytic bryophytes become highly abundant and diverse at higher altitude TMCF [3]. The peculiar hydroclimatic environment in TMCF associated with its fragmented nature also favors high levels of endemism. Gentry [2] estimates that 10-24% of the plant species in South American TMCF are endemic to this ecosystem. The species diversity and endemism in TMCF makes these ecosystems valuable gene pools for the improvement of commercial crop species [1] in addition, a high diversity of mammal, amphibian and bird species are found primarily in TMCF [3,16,17].

The low transpiration rates and high cloud water input in TMCF contribute to the maintenance of the streamflow in mountainous regions during the dry season [3,4]. The cloud water input in TMCF usually ranges from 15-20 % of the rainfall, but in some sites it can contribute as much as 50-60% [1]. The hydrological function of TMCF is important for the water supply of major cities in mountainous regions [1]. Besides its direct influence on streamflow, TMCF also acts to naturally filter water which contributes to a higher water quality in the streamflow [5].

Changes in climate and land-use are major threats to TMCF [16,18–20]. Model simulations predict that increases in land surface temperature could increase the height of cloud formation in tropical mountains [16,19,20]. Changes to TMCF cloud immersion regime holds major implications for its vegetation physiology and ecosystem processes [21–26], and its decline threatens the integrity of these ecosystems. The fauna of TMCF are also highly vulnerable to changes in the TMCF cloud regime [18]. Pounds et al [18] attributes the loss of 40% of the frog species in a Costa Rican TMCF to the increase in the number of days without rainfall or fog. Mountain environments are also subject to increased rates of climate warming [27]. Increases in temperature of up to 4° C are predicted to occur in TMCF [22•], which should aggravate the water deficit associated with the cloud uplift.

Predicting TMCF responses to climate change requires a mechanistic understanding of how TMCF hydroclimatic conditions determine its community composition and functioning. Functional traits provide a theoretical bridge to link plant physiological responses to environmental gradients/conditions and community assembly [28]. Information on plant functional traits can be incorporated into process-based Dynamic Global Vegetation Models (DGVM) to predict large scale vegetation shifts in response to climate change [29,30]. Whereas certain vegetation traits are widely associated with TMCF such as small and thick leaves that form canopies with low Leaf Area Index (LAI), and low

stature trees [6,8,16,31], little is known about more detailed aspects of TMCF photosynthetic and hydraulic functioning. This information is essential to predict plant responses to climate [32,33]. In this review we address this important knowledge gap by compiling functional trait data from TMCF communities. We use this functional trait information to characterize TMCF and understand what makes these communities functionally different from nearby forests not affected by clouds. In addition, we use the TMCF functional trait information to parametrize process-based models which are used to understand how the climate drives water transport, stomatal regulation and photosynthesis in the TMCF vegetation. The main questions we intend to address in this review are: i) What are the functional traits of the species that dominate TMCF and how do they differ from humid tropical forests not affected by clouds? ii) How do these functional traits modulate TMCF responses to climate? and iii) What mechanisms can explain the predominance of certain functional traits in TMCF? We also aim to identify critical knowledge gaps about TMCF which currently limit our capacity to respond these questions.

2. A case study of South/Southeast Brazilian Cloud Forest functional composition

We start this review with a case study focused on TMCF forest from South/Southeast Brazil (SSBCF) (Table 1; Fig. S1). We use floristic data from 10 TMCF sites and 8 non-cloud affected Atlantic forests sites in South/Southeast Brazil to illustrate the floristic and functional differences between TMCF and nearby non-cloud affected tropical forests. For this compilation we chose studies that fulfilled the following conditions: 1- the study was conducted within the area of interest (South/Southeast Brazil), 2- the study provided information on the species relative abundance, and 3 – the sites were classified either as Cloud Forests or Atlantic forests not affected by clouds. We use the term TMCF throughout the text to refer to tropical and subtropical montane forests exposed regularly to clouds, including Lower Montane Cloud Forests (LMCF), Upper Montane Cloud Forests (UMCF) and Elfin/Dwarf Cloud Forests [16]. All TMCF sites used in this section were located at altitudes higher than 1000 m and in locations frequently exposed to clouds (Fig. S1). The TMCF study sites have a mean annual temperature (MAT) on average 5° C lower than non-TMCF sites, with a MAT lapse rate of 0.4° C per 100 m (Fig. S2). The SSBCF sites were dominated by characteristic TMCF genera (Fig. S2), such as *Drymis*, *Ilex*, *Weinmannia* and several Myrtaceae genera [9,12,13]. The exceptions were the more northern sites, CF9 and CF10, which were dominated by Euphorbiaceae and Solanaceae (Fig. S3). We used genus (or family) level means of plant functional traits compiled from the Choat et al [34] and Kattge et al [35] datasets together with the species abundance at each site (Table 1, Fig. S3) to compute community weighted average (CWA) trait values for each studied site. See Appendix S1 for details on our methodology. This approach assumes the existence of a strong phylogenetical signal [36], which was found in most of the studied functional traits (Table 2). We adopted this indirect approach to circumvent the lack of functional trait data for Brazilian TMCF, which highlights the urgent need for more trait surveys in these forests. While these indirect CWA estimates must be interpreted carefully, we show in the next section they largely agree with published values collected *in situ* in TMCF worldwide.

We conducted a cluster analysis on the CWA traits using the first two principal axes from a Principal Component Analysis (PCA) to identify a possible functional convergence among these TMCF sites. The sites can be grouped into two clusters which maximize the data average silhouette width, that is, minimize the dissimilarity between points within a cluster [36] (Fig. 1). The blue cluster contains 8 out of the 10 TMCF sites used in this analysis

(Table 1). The main CWA traits that define the blue cluster sites are low Specific Leaf Area (SLA), low leaf nitrogen content on a mass basis (N_m), low sapwood specific hydraulic conductivity (K_s) and high Huber Value (HV). The sapwood density (ρ) is also lower in the blue cluster, but it is mostly associated with the within cluster variability along the second PCA axis. The red cluster contains all the Atlantic forest sites not affected by clouds in addition to the two most northern TMCF sites (CF9 and CF10). The different CWA in the northern TMCF sites reflects its floristic composition distinct from the other TMCF sites (Fig. S3).

The values of the functional traits predominant in SSBCF are associated with more conservative ecological strategies, that is, plants with slower rates of resource use and acquisition [37]. In the next section we assess the generality of this finding by contrasting the results from our indirect phylogenetic approach with data collected *in situ* from TMCF around the globe. We review sequentially the functional traits of TMCF leaves, wood and roots. Whereas, most of the discussion in the next sections is focused on the traits present in Fig. 1, other traits relevant to understanding TMCF functioning are also discussed.

3. Cloud Forest leaves and canopy

3.1. Leaf structure, stoichiometry and photosynthesis

The apparent xeromorphism of TMCF leaves has intrigued plant ecologists for several decades [6–8,38], given the humid TMCF environment, albeit the generality of this assumption is questionable as TMCF can occur across a wide range of rainfall regimes [38,39•] and high atmospheric aridity [40–42]. As expected, the dominant genera in SSBCF communities had leaves with an SLA 1.86 (CI95%: 0.01 to 3.72) $m^2\ kg^{-1}$ lower than non-TMCF communities (Fig. 1a). These findings are corroborated by numerous studies reporting a decline in SLA with increasing altitude in tropical mountains [10,43–45]. Kitayama & Aiba [44] have found a mean SLA of 4.95 and 3.98 $m^2\ kg^{-1}$ in two Bornean Upper Montane Forest sites, which were on average 2.61 $m^2\ kg^{-1}$ lower than nearby Lowland Rainforests (LRF). Van de Weg et al [10] reports a SLA of 7.47 ± 1.1 (mean±SE) $m^2\ kg^{-1}$ in four Peruvian TMCF sites, on average 4 $m^2\ kg^{-1}$ lower than a nearby LRF. According to Grubb [8] UMCF have SLA values ranging from 4.5 to 7 $m^2\ kg^{-1}$ and LMCF can reach 8 $m^2\ kg^{-1}$, while LRF ranges from 9 to 13 $m^2\ kg^{-1}$. The TMCF CWA SLA of 9.9 (CI 95%: 8.6 to 11.2 $m^2\ kg^{-1}$; Fig. 1a) for SSBCF are on the higher end of Grubb [8] and Van de Weg et al [10] observations. As noted by Bruijnzeel & Veneklaas [31], the lower SLA in TMCF makes its total leaf biomass closer to LRF, despite the large LAI difference between communities. The TMCF LAI can be as low as 2 $m^2\ m^{-2}$ in dwarf TMCF [46], but typically ranges from 5 to 6 $m^2\ m^{-2}$ in UMCF [8,31], while LRF LAI can reach 9 $m^2\ m^{-2}$ [8]. The leaf biomass (kg) per m^2 of soil in TMCF (computed as 1/SLA x LAI) ranges from 0.71 to 1.25 kg m^{-2} assuming an SLA between 4 and 7 $m^2\ kg^{-1}$ and a LAI of 5 $m^2\ m^{-2}$. This is potentially higher than LRF leaf biomass which should range from 0.69 to 1 kg m^{-2} assuming its SLA ranges from 9 to 13 $m^2\ kg^{-1}$ [8] and the LAI is 9 $m^2\ m^{-2}$.

SLA is the product of leaf thickness and density and is one of the traits at the core of the fast-slow continuum in plant ecological strategies [37,47]. A lower SLA implies a higher investment in structural and defense tissues, which increases the leaf resistance to herbivory and disturbances, resulting in a longer lifespan [47]. The low SLA in TMCF species, as well as many other TMCF traits are often attributed to low nutrient availability [11•,39•]. However, the

137 effect of nutrient availability on SLA is relatively small if compared with the effect of irradiance [48]. High irradiance
138 and atmospheric aridity can also explain TMCF leaf structure [40–42]. Smith & Geller [41] model simulations shows
139 that bigger leaves, which usually have higher SLA, would quickly overheat at higher altitude because of the higher
140 radiation loads. The thick cell walls, radial sclereids and fibres of low SLA plants allow the maintenance of cell turgor
141 during dehydration [49], which results in a more negative π_{tlp} [50]. However, the leaves from the dominant genera in
142 SSBCF lose turgor at similar Ψ than non-TMCF, around -2.15 MPa (Fig. 1b). Despite the weak phylogenetic signal
143 found in π_{tlp} (Table 2) our CWA π_{tlp} are within the range reported for TMCF and LRF. The value we estimated is in
144 the range of observations from TMCF in New Zealand, Colombia and Hawaii, which report a π_{tlp} ranging from -1.34
145 to -2.6 MPa [54–56]. Marechaux et al [54] reports a wider interval for 71 LRF species, with the π_{tlp} ranging from -1.4
146 to -3.2 MPa.

147 SLA is strongly correlated with leaf N_m and longevity, forming the classic leaf economic spectrum of Wright
148 et al [47]. The dominant genera in our TMCF sites follow this classic trade-off possessing on average 5.25 (CI95%:
149 2.19 to 8.33) mg g^{-1} less N_m than non-TMCF communities (Fig. 1c). Tanner et al [43] shows that leaf N_m declines at a
150 rate of 0.12 mg g^{-1} per 100 m increase in altitude across several tropical forest sites ranging from 0 to 3700 m of
151 altitude. Van de Weg et al [10] study over a 220-3360 m altitudinal gradient in Peru a shows a decline in leaf N_m of
152 0.26 mg g^{-1} per 100 m of altitude. Our observed leaf N_m decline rate of 0.4 mg g^{-1} per 100 m (Fig. 1b) is considerably
153 higher than both studies. Grubb [8] shows the N_m across several UMCF sites can range from 8.1 to 16.1 mg g^{-1}, while
154 LMCF can reach 17.6 mg g^{-1}. Soethe et al [45] found a leaf N_m of 15.5 ± 3.16 (mean±SE) mg g^{-1} for three Ecuadorian
155 TMCF sites. These values are close to our TMCF CWA N_m of 16.6 (CI95%: 14.2 to 19) mg g^{-1} (Fig. 1c).

156 Plants grown in lower temperatures typically have higher amounts of nitrogen-rich photosynthetic enzymes
157 to compensate for the lower activity of the enzymes at low temperatures [55]. Several studies report high leaf-level A_n
158 in TMCF species, which are close to non-pioneer LRF species A_n [31]. Letts & Mulligan [56] measured seven pairs
159 of congeneric species in a Colombian LMCF and UMCF. They have found light saturated maximum A_n of 10.6 and
160 10.2 µmol m^{-2} s^{-1} for the LMCF and UMCF, respectively. van de Weg et al [57] reports light saturated mean A_n rates
161 of 7.04 ± 0.33 (mean±SE) µmol m^{-2} s^{-1} for five TMCF species in Peru. Our findings for SSBCF are in agreement with
162 these studies, as the dominant genera in our TMCF sites have similar A_n to non-TMCF communities (Fig. 1d). The
163 TMCF CWA A_n was 9.93 (CI95%: 9.61 to 10.26) µmol m^{-2} s^{-1}, while non-TMCF communities CWA A_n was 10.26
164 (CI95%: 9.91 to 10.71) µmol m^{-2} s^{-1}. However, Wittich et al [58] reports the light saturated A_n of 170 species from 18
165 sites in altitudes ranging from sea-level to 4000 m decreases by 0.13 µmol m^{-2} s^{-1} per 100 m increase in altitude.

166 We can use the ratio between N_m and leaf phosphorus content (N:P) to assess nutrient limitations to plant
167 growth [59,60]. Aerts & Chapin [60] classifies a N:P ratio lower than 14 as indicative of N limitation, whereas N:P
168 higher than 16 indicates P-limitation. Gusewell [59] defines that leaf N:P lower than 10 or higher than 20 are indicative
169 of N and P-limitation, respectively. We did not have leaf P in the dataset used for the analysis of the SSBCF sites.
170 However, we compiled published data of leaf N:P from 31 LMCF and UMCF, six LRF and two subalpine sites, to
171 evaluate the evidence supporting the hypothesis of nutrient limitation in TMCF. We found no significant differences
172 in the leaf N:P among LMCF, UMCF and LRF (Fig. S4). There was also no relationship between leaf N:P and altitude

for the 19 sites where the altitude data was available (Fig. S4; R^2=0.07, p=0.23). Only two out of 15 UMCF sites showed sign of N limitation (i.e. N:P < 14), whereas 44% of the LMCF showed sign of N limitation. Only three LMCF sites had a N:P lower than 10, and they were all from Hawaii [61,62]. Despite our findings, some studies have experimentally demonstrated that TMCF productivity is limited by nutrients [11,43,63•]. As noted by Gusewell [64], as high altitude plants tend to have higher leaf N than low elevation plants, they might reach higher N:P ratios even in N-limited environments.

3.2. The role of leaves in water acquisition

An important characteristic of TMCF leaves which received considerable recent attention is the capacity of TMCF leaves to acquire directly the water condensed on its surface through foliar water uptake (FWU) [21,24,25,53]. This process is driven by a water potential (Ψ) gradient between the water outside leaves and the water inside, with the water flowing through the stomata [65,66], cuticle [24,67] and/or specialized structures [24,68]. Eller et al [24,25] showed through greenhouse experiments that FWU allows saplings of three Brazilian TMCF species to sustain gas exchange, leaf turgor and growth during soil drought. The total amount of water absorbed by FWU is small but not insignificant, ranging from 5 to 26 % of maximum transpiration fluxes [69]. Importantly, Goldsmith et al [21] reported a Ψ increment of 0.67 ± 0.02 (mean±SE) MPa in the leaves of 12 TMCF species after one hour of experimental leaf wetting, which was higher than the Ψ increment in a nearby submontane forest of 0.55 ± 0.12 (mean±SE) MPa. As noted by Oliveira et al [22•], this magnitude of water input and Ψ increment can be very important to maintain the hydraulic integrity and survival of plants in certain TMCF during seasonal and interannual droughts. However, Berry et al [69] show that FWU is a ubiquitous process found in plants worldwide, including LRF [70]. Binks et al [70] observed a mean leaf Ψ increment in Amazon tree species of 0.63 MPa after one hour of artificial wetting, which is close to observations of Goldsmith et al [21] for TMCF. More studies are necessary to understand the differences between the occurrence and significance of FWU for LRF and TMCF. Whereas TMCF can likely benefit from high FWU rates due to the persistence of cloud immersion events wetting its canopy, Dawson & Goldsmith [71] show that plants in most biomes in the world are also exposed to long periods with wet leaves, including LRF.

Oliveira et al [22] note that the ecophysiological importance of FWU to TMCF plants varies from site to site and seasonally. Whereas most TMCF occurs in sites with high rainfall (2000 to 2600 mm from Jarvis & Mulligan [39•]), a significant number of TMCF sites might occur in lower rainfall locations. Jarvis & Mulligan [39•] show that 6 % out of 477 TMCF sites from the UNEP-WCMC global database (UNEP-WCMC, 2004) occur in locations that receive less than 1000 mm of rainfall annually. Some sites receive as little as 405 mm annually and can be exposed to significant rainfall seasonality. Additionally, the shallow soils usually found in TMCF [72,73] coupled with a potentially high atmospheric aridity due to higher incident shortwave irradiance and diffusivity of water vapor and heat in air [40–42] can cause water shortage for TMCF plants during seasonal or interannual periods with reduced rainfall. Mortality events in TMCF vegetation have been reported following severe droughts [74,75]. These conditions make the vegetation in drier TMCF sites highly dependent on cloud water input, both through direct cloud interception and FWU, to sustain its physiological activity during the dry season [26,76–78]. Acquiring the water condensed on

the plant canopy through FWU before it drips to the forest floor is a method to bypass the belowground competition for water with other plants, and the possibility of interception by epiphytes and understory vegetation.

The TMCF arboreous component should only experience water stress regularly in more arid TMCF sites. However, the epiphytic community of every TMCF regularly experiences water stress due to the limited soil volume available and high radiation in the canopy environment [79]. Gostch et al [23] shows that FWU provides large amounts of water to some epiphytes in a Costa Rican TMCF. During one month of observations, the seven epiphyte species studied by Gostch et al [23] absorbed through FWU on average 70 % of its transpired water, with some species absorbing up to 96 % of its transpired water. Not all epiphytes are capable of FWU [68], therefore more studies are necessary to assess the FWU capabilities of different TMCF epiphytes. The epiphytic community is an essential component of TMCF water and nutrient cycles [16,79], and its reliance on FWU makes this process extremely important for TMCF functioning.

Besides acquiring water through FWU, TMCF leaves might also contribute to the plant nutrient acquisition through N foliar uptake [80]. Cloud water from forests in Southern Chile can contain significant amount of organic and inorganic N [81]. Additionally, the canopy of TMCF hosts microbes and epiphytes capable of fixing atmospheric N_2 [82,83]. We postulate that plants capable of accessing these resources through direct FWU would have an important competitive advantage in N-limited TMCF. We could not find any studies on the relevance of FWU for nutrient uptake in TMCF, therefore we consider this topic a priority for future TMCF research.

4. Cloud Forest sapwood structure and hydraulics

4.1. Resistance to embolism and hydraulic safety

Contrary to TMCF leaves, which possess well-defined characteristics differentiating them from LRF, much less is understood about the structure and function of TMCF wood. Wood functional traits, particularly the hydraulics of xylem (vessel and tracheid based), are a fundamental aspect of plant physiology which determine plant responses to climate [32,33,84]. The scarcity of studies investigating the hydraulic traits of TMCF communities is a major gap in our understanding of TMCF ecophysiology and limits our capacity to predict their response to climate change. In this section we compiled the available studies on this topic together with the functional analysis of SSBCF to provide an initial picture of TMCF wood hydraulic/functional traits.

The Ψ when the vessels or tracheids loses 50 % of its maximum hydraulic conductivity (Ψ_{50}) can be used as reference for the plant capacity to withstand drought-induced embolism [34,85]. The Ψ_{50} of evergreen plants is often positively related with plant water availability [86,87]. We did not detect significant differences between the Ψ_{50} of the dominant genera in SSBCF and non-TMCF communities (Fig 3e). Most studies assessing *in situ* branch xylem Ψ_{50} values of TMCF species have found values similar to our TMCF CWA Ψ_{50} of -2.54 (CI95%: -2.29 to -2.79) MPa (Table S1). In Oliveira et al [22•] we reported a Ψ_{50} for the vesselless angiosperm *Drimys brasiliensis* located in CF7 (Fig. S1) of -1.56 MPa. More recently, Eller et al [88] measured the Ψ_{50} of seven additional TMCF species at the same site and found a Ψ_{50} of -2.79 ± 0.37 (mean±SE) MPa across all species. Hacke et al [89] and Sperry et al [90] conducted studies on vesselless and basal angiosperm hydraulics, and measured the Ψ_{50} of 12 TMCF species from Costa Rica,

243 New Caledonia and the North of Australia. Pooling together the TMCF species from these two studies results in a Ψ_{50}
244 of -2.42 ± 0.27 (mean±SE) MPa.

245 Plant K_s loss is traditionally described using a sigmoidal function with two parameters, such as:

246 $$\frac{K_s}{K_{smax}} = \frac{1}{[1 + (\Psi/\Psi_{50})^a]} \qquad (Eqn\ 1)$$

247 Where, the K_{smax} is the xylem or tracheid maximum K_s and a determines the shape of the curve. A low a implies K_s
248 starts declining at lower Ψ but with a small K_s loss rate, so $K_s > 0$ even when Ψ is much lower than the Ψ_{50}. A high a
249 will produce a clear Ψ threshold at Ψ_{50} where the plant suddenly shifts from $K_s \approx K_{smax}$ to $K_s \approx 0$. There is considerable
250 variation in the shape of vulnerability curves in plants globally [91], which implies that the Ψ_{50} by itself does not
251 provides a complete picture of xylem or tracheid resistance to drought induced embolism [92]. Despite the importance
252 of the vulnerability curve shape for modelling plant hydraulic and stomatal functioning [32,33] few studies report this
253 quantity. We could not find a single published a value for a TMCF species in the literature. We used published
254 vulnerability curve data from the eight TMCF species from Eller et al [88] to compute the linear gradient between Ψ_{50}
255 and the Ψ where K_s loses 88 % of its K_{smax} (Ψ_{88}), and compared this gradient with the gradient from LRF using 13 tree
256 and shrub species from the Choat et al [34] dataset. We have found similar gradients between communities, with the
257 TMCF species K_s/K_{smax} dropping 0.32 (CI95%: 0.13 to 0.52) per MPa, while the LRF species K_s/K_{smax} would drop
258 0.33 (CI95%: 0.18 to 0.49) per MPa. Clearly more data on the vulnerability curve shape is needed before we can make
259 firm conclusions about how the plants of these communities lose K_s in response to drought. Based on the currently
260 available data, TMCF and LRF species vulnerability to embolism are remarkably similar, both in shape and Ψ_{50} (Fig.
261 1d).

262 There was a gradual increase in the leaf minimum Ψ (Ψ_{min}) with altitude at a rate of 0.01 MPa per 100 m
263 increase in altitude in the SSBCF sites (Fig. 1f). This increment rate implies that at our highest TMCF site at 2250 m
264 trees would have a xylem hydraulic safety margin (HSM, calculated as $\Psi_{min} - \Psi_{50}$) of 0.54 MPa, which is 0.45 MPa
265 higher than at sea-level, assuming the communities have their respective mean Ψ_{50} from Fig. 1d. There are very few
266 studies reporting HSM values for TMCF, but Eller et al [88] have found a mean HSM of 1.31 ± 0.24 MPa which is
267 substantially higher than the global tropical forest HSM median of 0.33 MPa (Choat et al [34]). These observations
268 can be interpreted as evidence that some TMCF rely on a more conservative stomatal regulation to maintain a high Ψ,
269 relative to its Ψ_{50}, resulting in a relatively large HSM.

270 *4.2. Hydraulic efficiency and architecture*

271 While some TMCF communities might possess a safer hydraulic system (i.e. higher HSM) when compared
272 with LRF communities, the TMCF hydraulic system is generally less efficient when expressed on a sapwood basis.
273 We found that the dominant genera in SSBCF TMCF had a K_s on average 0.97 (CI95%: 0.12 to 1.81) kg m^{-1} s^{-1} MPa^{-1}
274 lower than non-TMCF communities (Fig. 1g). The low K_s in TMCF can be partly attributed to the abundance of
275 vesselless basal angiosperms in the TMCF community, such as *Drimys*, and other species with primitive vessel

morphology, such as *Weinmannia*, which have high sapwood specific resistivity [89,90]. Zotz et al [93] found that trees in a Panamanian TMCF have sapwood hydraulic conductivity, expressed on a leaf area basis, 0.08 to 1.4 kg m^{-1} s^{-1} MPa^{-1} lower than LRF trees. In terms of absolute values, Feild & Holbrook [94] have found K_s varying from 0.12 to 0.65 kg m^{-1} s^{-1} MPa^{-1} in eight TMCF species. These values are considerably lower than our TMCF CWA K_s of 1.97 (CI95%: 1.28 to 2.65) kg m^{-1} s^{-1} MPa^{-1} (Fig. 1g). Low K_s is associated with conduits of smaller diameters [95], as explained by Poiseuille's law. Small diameter conduits are more resistant to ice nucleation [96], which might indicate a temperature mediated selection on TMCF hydraulic traits. Freezing temperatures can occur in some TMCF [39•,97] and potentially induce freeze-thaw embolism in species with wider conduits.

The TMCF hydraulic architecture is also distinct from non-TMCF communities (Fig. 1h-i). The dominant genera in South/Southeast TMCF possess, on average, 1.68 (CI95%: 0.57 to 2.5) cm^2 more sapwood area per leaf area (i.e. HV) than non-TMCF communities (Fig. 1h). The difference in HV between TMCF and LRF species have been reported previously in the literature [93,98]. Zotz et al [93] reports TMCF trees have on average 3 cm^2 more sapwood area per m^2 of leaf area than LRF. Santiago et al [98] have found an TMCF population of *M. polymorpha* had 0.4 cm^2 more xylem area per m^2 of leaf area than a LRF population. The HV computed for the eight TMCF species by Field & Holbrook [94] range from 5.3 to 20.8 cm^2 m^{-2} which are above our TMCF CWA HV of 3.77 (CI95%: 2.94 to 4.6) cm^2 m^{-2} (Fig. 1h) and might reflect the weak phylogenetic signal on HV (Table 2).

The length of the hydraulic path linking root and leaves, which is associated with the tree height, is another important aspect of tree hydraulic architecture [99,100]. Low tree stature is a defining characteristic of TMCF vegetation [8,16]. Accordingly, we have found that the SSBCF communities are composed by genera with a significantly lower H_{max} than non-TMCF communities (Fig. 1i). The mean difference in H_{max} between TMCF and non-TMCF is 4.28 (CI95%: 0.97 to 7.6) m, with a TMCF CWA H_{max} of 19.45 (CI95%: 16.6 to 22.2) m. Our observations fall within the TMCF tree height interval defined in the literature as ranging from 1.5 to 20 m [4,8,31].

The low stature of TMCF trees associated with its higher HV results in a higher tree height-diameter ratio than LRF [63•]. This type of tree architecture is also observed in trees exposed to intense mechanical perturbations [101,102]. Strong winds are common in high-altitude environments, being particularly common in TMCF located in exposed ridges [72,73,102,103] and Arriaga [72] shows that wind is a major cause of vegetation mortality in TMCF. Therefore thigmomorphogenetic response in TMCF vegetation, that is, the plant growth patterns shift to increase its capacity to withstand mechanical perturbations [101,102] is another possible explanation for the TMCF stunted architecture.

The effect of strong winds on trees also depend on its wood properties [103–105]. Higher wood density (ρ) provides a better combination of elasticity and mechanical strength for wood to withstand high winds [103–105]. However low ρ allows trees to produce thicker trunks for a given height with a smaller carbon investment, which are more resistant to wind damage [104]. The dominant genera in SSBCF have wood slightly less dense than non-TMCF communities, with ρ decreasing 0.0025 g cm^{-3} per 100 m increase in altitude (Fig. 1j). Despite our data showing a weak (but statistically significant) relationship, Chave et al [106] shows a similar negative relationship between ρ and altitude in a large-scale study with 2456 Neotropical tree species. A lower ρ implies TMCF species can rely on an

312 increased diameter/height ratio to resist wind damage. Several studies report tree diameter/height ratio increases with
313 altitude (see Fahey et al [133] for a review), which corroborates this hypothesis.

314 **5. Cloud Forest roots**

315 There are considerably less studies investigating the belowground traits of TMCF than its aboveground traits,
316 which reflects the technical and logistic challenges of measuring belowground traits and processes. However, the
317 observations available indicate TMCF allocate a large fraction of its assimilated carbon to root production [8,44,107–
318 109], indicating belowground organs have a central role in TMCF. We had no root related information in the dataset
319 used for the SSBCF analysis, therefore we focus this section on compiling data available in the literature regarding
320 the structure and function of TMCF roots.

321 According with Grubb [8] TMCF can reach a belowground biomass from 40 to 72 Mg C ha^{-1}, whereas LRF
322 ranges from 11 to 67 Mg C ha^{-1}. According with this Grubb [8] data, the ratio of belowground to aboveground biomass
323 in TMCF is 0.27, which is more than twice the LRF ratio (0.12). Similarly, Girardin et al [108] found the fine root to
324 stem biomass ratio increases from 0.02 at 194 m to 0.11 at 3020 m across an altitudinal gradient in Peru. Leuschner
325 et al [107] observed even greater carbon allocation changes in Ecuadorian montane forests, with the root to
326 aboveground biomass ratio increasing from 0.04 at 1050 m to 0.43 at 3060 m.

327 The increased belowground carbon allocation in TMCF is often attributed to a nutrient limitation on plant
328 growth [11•]. Plants tend to allocate carbon in order to maximize the acquisition of limiting resources [110], therefore,
329 N or P limitations tend to increase plant root:shoot ratio [111]. There is some evidence that the fine roots of TMCF
330 possess morphological traits to facilitate nutrient acquisition [112]. Girardin et al [112] shows that Peruvian Andes
331 TMCF have a higher specific fine root area (SFRA) and specific fine root length (SFRL) than LRF forests from
332 Metcalfe et al [113]. Higher SFRA and SFRL allow plants to explore a bigger volume of soil per mass of carbon
333 invested in root production. However, other mechanisms might also favor high SFRA and SFRL, such as a denser soil
334 structure [114] or a decrease in root herbivory [115]. Lower temperatures can decrease root nutrient uptake capacity
335 [116,117], therefore the higher investment in fine roots for nutrient acquisition can compensate for a lower nutrient
336 absorption rate per unit of root area.

337 A higher biomass allocation to roots can also be attributed to increased need for mechanical stability in the
338 TMCF environment. Higher-altitude TMCF sites usually have a higher proportion of uprooted and snapped trees than
339 lower elevation sites [72,73]. Soethe et al [73] have found that the coarse roots from an Ecuadorian elfin forest are
340 more asymmetrical and expand more horizontally in the soil than trees at lower altitudes. These coarse root
341 morphological traits improve tree capacity to withstand the irregular mechanical loads associated with the TMCF
342 shallower and unstable soils, steep slopes and strong winds [73]. In addition to the wind and the tree's own weight,
343 the TMCF root system needs to support a considerable biomass of epiphytes and associated canopy humus [118,119].
344 Hofstede et al [119] reports that a single *Weinmannia mariquitae* tree in a Colombian UMCF would hold 115 kg of
345 epiphytic biomass, which was equivalent to 12% of the tree biomass. The total epiphytic mat weight on an area basis
346 can reach up to 44 Mg ha^{-1} in UMCF [119].

6. Environmental drivers of carbon and water fluxes in Cloud Forests

6.1. Climatic controls on leaf-level photosynthesis

In this section we use the functional traits compiled previously to parametrize a photosynthesis model [120] for TMCF vegetation and evaluate the main abiotic factors controlling TMCF A_n. A very clear pattern observed in the TMCF functional traits is the decline of SLA and leaf N_m at increasing altitudes (Fig. 1). As SLA decreases with increasing altitude (Fig. 1a), less N_m is necessary to achieve a given N content per leaf area (N_a). This makes leaf N_a less sensitive to altitude changes than N_m, and in some cases it might be even higher in TMCF than in non-TMCF communities [10,44]. This distinction is important to understand the mechanisms controlling TMCF leaf-level carbon assimilation, as the maximum rate of Rubisco carboxylation at 25° C (V_{cmax25}) is a linear function of N_a [121]. Using the intercept and slope values for tropical trees from Harper et al [122] and the CWA N_a from Fig. 1 (i.e. $N_a = N_m$ x 1/SLA), we estimate a mean V_{cmax25} for TMCF of 40.48 µmol m^{-2} s^{-1}, which is just 2.9 µmol m^{-2} s^{-1} lower than the non-TMCF mean V_{cmax25}. Our TMCF V_{cmax25} estimates are lower than the V_{cmax25} of 55.6 ± 23.03 (mean±SD) µmol m^{-2} s^{-1} measured by van de Weg et al [57] in a Peruvian TMCF, which is higher than the V_{cmax25} typically found in LRF [123–125]. This pattern can be interpreted as one type of acclimation of the plant photosynthetic apparatus to lower temperatures. These findings suggest that it is unlikely that TMCF A_n is limited by its V_{cmax25}. To understand how abiotic factors controls TMCF A_n, we used the Collatz et al [120] photosynthesis model to simulate TMCF A_n responses to altitudinal gradients (Fig. 2). The A_n of C_3 plants can be described as the minimum of three limiting processes, the Rubisco carboxylation capacity (J_c), the light-dependent Rubisco regeneration (J_l), and the capacity to export or utilize the photoassimilates (J_e). These processes can be represented following Collatz et al [120]:

$$A_n = min\begin{cases} J_c = V_{cmax}\left[\dfrac{c_i - \Gamma}{c_i + K_c(O_a/K_o)}\right] \\ J_l = \alpha(1-\omega)I_{par}\left(\dfrac{c_i - \Gamma}{c_i + 2\Gamma}\right) - R_d \\ J_e = 0.5V_{cmax} \end{cases} \qquad (Eqn\ 2)$$

Where V_{cmax} is the temperature adjusted Rubisco maximum carboxylation rates, c_i is the leaf internal CO_2 concentration, Γ is the photocompensation point, K_c and K_o are Michaelis-Menten constants for CO_2 and O_2, respectively, O_a is oxygen partial pressure in the atmosphere, α is the intrinsic quantum efficiency of CO_2 uptake, ω is the leaf light scattering coefficient, I_{par} is the photosynthetically active radiation incident on the leaf and R_d is the leaf dark respiration. Our simulations indicate that at higher altitude A_n tends to be limited by temperature effects on J_c or J_e (Fig. 2). Cloudiness in TMCF can reduce I_{par} (Fig. S1) which limit A_n in lower altitudes, but even a reduction of 90% in the I_{par} is not enough to reduce J_l to lower levels than J_c and J_e at higher altitudes TMCF (Fig. 2b-d). Bittencourt et al [126] shows that fog and rain events attenuate, on average, from 74 to 80% of the incoming radiation in a SSBCF, therefore our simulations represent a particularly strong cloud effect on I_{par}. It is important to note that the leaf wetting associated with rain and fog can have a stronger effect on leaf A_n than what we can predict with equation 1. Leaf wetting can directly restrict the CO_2 diffusion to the leaf interior, due to the formation of a water film over the stomata [56,127]. This effect would reduce plant c_i affecting J_c and, to a lesser extent, J_l.

The total effect of changes in CO_2 partial pressure with altitude on A_n are very small (Fig. 2b). The decline in the atmospheric CO_2 partial pressure is mostly compensated with a lower O_a in J_c, which decreases Γ (computed as $O_a/2\tau$ after Collatz et al [120]), where τ is the Rubisco affinity for CO_2 relative to O_2). The modelled decrease in J_c or J_e which dominate A_n responses to altitude is caused by the temperature effects on V_{cmax25} (Fig. 2a). The V_{cmax} value used in equation 1 is calculated as a function of V_{cmax25} and leaf temperature (T_l) following Clark et al [128]:

$$V_{cmax} = \frac{V_{cmax25}\left[2^{0.1(T_l-25)}\right]}{\left[1+e^{0.3(T_l-T_{upp})}\right]\left[1+e^{0.3(T_{low}-T_l)}\right]} \quad (Eqn\ 3)$$

Where T_{low} and T_{upp} are the parameters that define the lower and upper limits of V_{cmax}. The T_{low} and T_{upp} for evergreen broadleaved tropical trees is 13° and 43° C according to Harper et al [122], which implies that Rubisco operates at its maximum efficiency when T_l = 39° C (Fig. 2a). Plants can adjust their photosynthetic apparatus to lower or higher temperature through changes on enzymes content and structure [55,129]. Given the large difference in MAT between TMCF and LRF (Fig. 2; S2) it is likely that TMCF species would have different optimum temperatures for Rubisco activity than LRF species. However, we could not find studies measuring the response of TMCF photosynthetic parameters to temperature, which imposes a major constraint on our capability to simulate TMCF A_n. We used the linear relationship between V_{cmax} and MAT from Kattge & Knorr [129] to estimate the optimum V_{cmax} temperature for cold acclimated TMCF plants at 2250 m. This approach predicts that plants acclimated for the TMCF lower temperatures would have an optimum V_{cmax} at 31°C. The acclimation of V_{cmax} temperature responses makes TMCF A_n decline only 0.02 μmol m^{-2} s^{-1} per 100 m increase in altitude, whereas if we assume no acclimation the decline rate reaches 0.17 μmol m^{-2} s^{-1} per 100 m (Fig. 2b). This large difference highlights the need for data on the TMCF V_{cmax} temperature responses so that the TCMF A_n can be correctly represented in vegetation models [130]. According to our simulations cold-acclimated TMCF leaves should be capable of reaching high A_n under favorable climatic conditions. However, the frequent leaf wetting events restrict the amount of time TMCF leaves are close to their optimum A_n [56].

Our simulations indicate that J_e and J_c co-limit TMCF A_n at higher altitude (Fig. 2). However, the limiting effect of J_e could be underestimated by our simulations. The J_e equation from the Collatz et al [120] model does not explicitly represent the effects of phloem functioning on the export of photosynthetic products from the leaves [131]. Phloem transport rates are dependent on the sap viscosity, which increases at low temperatures [132,133]. Besides, the sink activity of plant meristematic tissues is strongly inhibited by lower temperatures [134]. As plant growth is interrupted, phloem unloading and transport rates should decline, which can make temperature limitations on A_n at higher altitude more important than what can be predicted in our simulations with equation 2.

6.2. Stomatal responses to climate

The previous section shows the environmental controls on the biochemical and photochemical processes of A_n. In this section we focus on the role of stomatal responses to climate controlling plant carbon assimilation and hydraulic safety in TMCF. We used the leaf and hydraulic traits from Fig. 1 to parameterize a stomatal optimization model based on Eller et al [33] (full description in Appendix S2). The main assumption of the Eller et al [33] model is that plant stomata evolved to balance instantaneous A_n with the loss of hydraulic conductance, derived from

equation 1. The model predicts that both TMCF and non-TMCF plants will adopt a more conservative stomatal regulation at higher-altitude climate (Fig. 2). The modelled g_s response to soil and atmospheric drought is very similar between TMCF and non-TMCF plants, with TMCF reaching a slightly higher g_s than non-TMCF, especially at a low altitude environment (D; Fig. 2a-b). Even so, the TMCF leaf Ψ is similar to non-TMCF (Fig. 2c-d) due to its higher HV and low tree height, which compensates for its low K_s (Fig. S4). TMCF plants at high-altitude have a g_s, on average, 40% lower than at sea-level, while non-TMCF g_s is, on average, 32% lower at high altitude. This low g_s results in a higher leaf Ψ and HSM at high-altitude, which is partially supported by our observations (Fig. 1f). Whereas at sea-level the TMCF leaf Ψ reaches its Ψ_{50} when D = 1.6 kPa, at high-altitude it would still maintain an HSM of 0.85 MPa even at the highest simulated D at 2250 m (1.9 kPa). Similarly, in response to soil drying the model predicts that at low-altitude plants would always maintain a smaller root to leaf Ψ gradient, except during extreme drought, that is at root $\Psi \approx$ -3 MPa (Fig. 2d). At higher altitude, TMCF leaf Ψ would reach its Ψ_{50} when root Ψ = -2 MPa, whereas at sea-level TMCF would reach HSM = 0 with a root Ψ 0.5 MPa higher.

The conservative stomatal behavior predicted by the model can be attributed to the temperature response of V_{cmax25} (Fig. 2a), which decreases the potential A_n for a given g_s. The lower rates of carbon assimilated at high elevation do not compensate for the hydraulic conductance lost, resulting in a more conservative stomatal regulation. Our simulations assume no acclimation in the V_{cmax} response to temperature, an acclimation of the magnitude as the one shown in Fig. 2a would result in a similar stomatal behavior at low and high altitudes. A more conservative water use and stomatal regulation have been observed in many TMCF sites [24,51,52,135,136], but there is also evidence of TMCF species that respond very little to drought [137]. As discussed in the previous section and in Oliveira et al [22•] it is important to consider the role that FWU can have on maintaining the leaf Ψ in certain TMCF plants during drought. The water acquired by FWU might compensate for a less conservative stomatal regulation in some TMCF species and contribute to the maintenance of leaf turgor [24] and a higher HSM [22•].

6.3. Climatic limitations to water transport

In many species the HV increases with tree height to compensate for the increased hydraulic resistance caused by the increased distance between roots and leaves [99]. Our results indicate that TMCF are an exception to this trend as they have both low H_{max} and high HV (Fig. 1). McDowell et al [99] uses a simple hydraulic model based on Darcy's Law to explain why HV declines in taller trees:

$$HV = \frac{H\eta g_w D}{p_s \Delta\Psi} \qquad (Eqn\ 4)$$

Where p_s is the sapwood permeability, $\Delta\Psi$ is the soil to leaf Ψ gradient accounting for the gravitationally induced Ψ drop, H is tree height, η is water viscosity, g_w is the combined g_s and boundary layer conductance to water. This model predicts that, assuming all other parameters are constant, sustaining a given g_s at increasingly high H requires a higher HV (Fig. 3). We can use equation 4 to understand the differences in HV between TMCF and non-TMCF communities based on the biotic and environmental differences between these communities. The colder temperatures observed in TMCF [39•] cause η to increase from 9.54 x 10^{-4} Pa s at sea-level (MAT = 22.2° C) to 1.19 x 10^{-3} Pa s at our highest

site at 2250 m (MAT = 13.2° C). The increased viscosity restricts xylem water transport and requires more sapwood per leaf area (higher HV) to sustain a given g_s. While the lower temperature at higher elevations reduce air D (assuming constant air humidity), the increases in solar irradiance and water vapor diffusion coefficient can counteract the temperature effect [40–42]. We included a boundary layer and leaf energy budget model on the D calculation in Equation 4 to account for these effects (equations S2-S4 in Appendix S2). Equation 4 shows that the high-altitude TMCF environment requires a higher investment in HV to sustain a given g_s than the LRF environment (Fig. 3). An increase in 1 m in tree height will require 0.027 cm^2 more sapwood per m^2 of leaf to sustain a g_s = 1 mol m^{-2} s^{-1} in the high-altitude TMCF environment than at sea-level (Fig. 3). When we include the functional differences between TMCF and LRF (Fig. 1) in equation 4, the investment in sapwood per unit of leaf area becomes even more important for TMCF plants. The lower K_s in TMCF (Fig. 1g) and more conservative stomatal regulation (Fig. 2) results in a less negative Ψ_{min} (Fig. 1f). This makes an increase in 1 m in TMCF tree height require 0.15 cm^2 more sapwood per m^2 of leaf area in comparison with LRF to sustain a g_s = 1 mol m^{-2} s^{-1} (Fig. 3).

7. Abiotic filters shaping Cloud Forest communities

In the previous sections we described TMCF functional composition (Fig. 1) and the consequences of these traits for TMCF ecophysiological processes (Fig. 2-3). In this section we propose hypotheses to explain why these particular traits and processes are prevalent in TMCF vegetation. We employ the concept of environmental filters [138] to explain how the peculiar TMCF hydroclimatic environment selects a set of plant traits, which, ultimately, determine the functioning of TMCF ecosystems and its response to global change. We represent the postulated environmental filters in TMCF as a conceptual model in Fig. 4, which can provide a roadmap for the representation of TMCF in DVGM.

The concept of environmental, or abiotic, filter assumes the environment functions as a metaphorical "sieve" that only allow species with certain traits to establish and persist [148]. We postulate that lower temperatures are a fundamental environmental filter in TMCF (Fig. 4). Temperature will directly affect several TMCF plant processes, besides indirectly driving other important abiotic filters in TMCF, such as clouds and nutrient availability (Fig. 4). Lower temperatures favor cloud formation, due to its effect on the lifting condensation level (Fig. S2). Lower temperatures also decrease the soil nutrient availability by affecting nitrogen mineralization rates [139], besides directly affecting root nutrient uptake capacity [116,117]. Air temperature also affect directly many aspects of TMCF plant physiological processes, such as reducing the leaf A_n of non-acclimated species (Fig. 2), and making xylem and phloem transport more difficult due to its effect on water viscosity [132,133]. These effects can trigger a series of compensatory traits, such as a more conservative stomatal functioning (Fig. 2), a higher allocation to wood production over leaf area (Fig. 1h) and shorter path lengths between leaves and roots (Fig. 1i) to facilitate the canopy water supply. In colder TMCF sites temperature can have an even stronger selective effect on the community hydraulic traits. The occurrence of colder winters that can freeze xylem/tracheid water, even if rare, could have a lasting impact on TMCF community. Freezing induced embolism could favor species with small diameter and low conductivity xylem/tracheids (Fig. 1g) which are resistant to freezing embolism [96].

The persistence of cloud immersion events and low nutrient availability form another important layer of TMCF abiotic filters (Fig. 4). The occurrence of cloud immersion might favor competitively species capable of accessing and utilizing the resources made available by the frequent leaf wetting events (water and potentially nutrients), as well as select against species vulnerable to leaf pathogens. Leaf wetness favors the establishment of bacteria, fungi and other organisms which might damage leaves [71], therefore species with low structural investment on leaf tissues (high SLA) would be more vulnerable to leaf infection [140]. The leaf wetness associated with cloud immersion events also limits leaf A_n and can constrain the occurrence of fast acquisitive species [37,47], that is, species with both high A_n and SLA. Species with a fast leaf tissue turnover would depend on high A_n to quickly compensate its low carbon investment on its short-lived leaves. However, even though TMCF vegetation can potentially reach high A_n when climatic conditions are favorable due to its high leaf N content and V_{cmax25} (Fig. 1-2), it cannot consistently maintain a high A_n due to temperature related limitations on A_n (Fig. 2) and the frequent wet leaves interrupting leaf gas exchange [56,127]. The low nutrient availability in TMCF will also favor low SLA species [141] and species capable of sustaining a high investment in root production [110,111].

Besides the postulated main filters represented in Fig. 4, we propose other TMCF typical environmental conditions reinforce the selective effect of lower temperatures, clouds and low soil fertility. During clear periods, high-altitude environments are exposed to high levels of shortwave irradiance [41,42], which select against larger leaves with high SLA and more prone to overheating [41]. Higher transpiratory rates could provide an alternative mechanism to cool down leaves [142]. However, the limitations to water transport and stomatal regulations discussed previously prevent this strategy. Mechanical stress can also be a strong driver of plant form and function in certain TMCF [101,102]. Wind-induced stress can trigger thigmomorphogenetic responses that include low SLA, low tree stature (Fig. 1i) and high stem diameter/height ratio [143–145]. The existence of multiple independent environmental conditions selecting a similar set of traits can increase the resistance of the TMCF community to certain changes on environmental conditions. For example, traits such as low SLA would still be dominant in a TMCF community even in a site protected from wind, as the high irradiance and leaf wetting events would still favor low SLA species.

Multiple overlapping environmental filters can enhance TMCF resistance against certain types of environmental change, but the interactions between key TMCF environmental factors, such as temperature, cloudiness and nutrient availability (Fig. 4), make TMCF highly vulnerable to hotter climates. General circulation models predict an increase in the TMCF MAT from 2 to 4 °C in the next decades [22•]. A higher surface temperature can increase the cloud base formation height up to 1634 m in some TMCF sites [23]. An increase in 4 °C also would increase the litter decomposition and nutrient mineralization rates by 53% [139]. It is unlikely that TMCF communities could resist the simultaneous removal of the three main filters shaping their structure and driving their processes (Fig. 4). The lack of leaf wetting and higher temperatures events would allow plants to sustain a consistently high A_n, and the increased nutrient availability would decrease the need for high fine root investments. These changes can make TMCF environments more favorable to larger LRF species with highly acquisitive traits and fast tissue turnover. On this scenario, the current TMCF community would be restricted to higher altitude elevations [16], where the strength of other TMCF filters, such as high irradiance loads and water vapor diffusion on air [40–42] compensate for the higher

518 temperature and less clouds. Particularly windy TMCF sites with shallow soils and steep slopes could also be refugia
519 for TMCF communities, as they would still impose mechanical restrictions to the establishment of larger and fast
520 growing LRF species. However, even these sites can be invaded by grassland species and tropical shrubs, which can
521 thrive in drier sites [146]. These hypotheses can subsequently be tested in a process based DGVM framework using
522 the data presented here to represent TMCF vegetation.

523 Abiotic filters are not the only elements determining the structure and function of ecosystems. Biotic
524 interactions and dispersal limitations often have a significant role on community assembly [147]. These effects are
525 important for understanding TMCF dynamics, especially due to the role of epiphytes in TMCF biogeochemistry [76].
526 The epiphytic community of TMCF is exposed to a more arid environment in the canopy than the rest of the TMCF
527 community [79], therefore it should respond faster to a decrease in cloud immersion and increased temperatures.
528 Declines on the epiphyte's abundance can accelerate TMCF responses to climate change by decreasing TMCF cloud
529 water interception and nutrient acquisition combined with changes in the canopy fauna. A decrease in the heavy
530 epiphytic load characteristic of TMCF will also decrease the need for investment resources to increase the tree
531 mechanical stability, which should facilitate the establishment of species with a typical LRF architecture.

532 **8. Conclusions**

533 Our findings show that the unique hydroclimatic conditions in TMCF selects a community functionally
534 distinct from other tropical forests (Fig. 1), which results in different ecophysiological responses to climate (Fig. 2-3).
535 The TMCF functional composition can be interpreted as the result of many interacting and overlapping environmental
536 filters (Fig. 4). These filters impose restrictions on the establishment of larger and fast-growing lowland species
537 through hydraulic and mechanic restrictions on plant height (Fig. 3), coupled to temperature and leaf-wetting related
538 restrictions on leaf structure, stomatal functioning and carbon assimilation (Fig. 1-2). The TMCF community also
539 have proportionally large root systems with a high density of fine roots, which reflects a heavy investment on nutrient
540 acquisition.

541 The functional uniqueness of TMCF we show on this review must be considered in DGVM and Earth System
542 models to quantify the potentially large contributions of this ecosystem global and regional biogeochemical cycles
543 and climate [148]. Our conceptual framework based on TMCF functional traits (Fig. 4) suggests that TMCF structure
544 and function are highly vulnerable to increases in temperature, which are likely to occur in the next decades [22,27].
545 Our findings provide a roadmap for the inclusion of TMCF in DGVMs, which should enable the assessment of TMCF
546 vulnerability to climate change scenarios at the global scale. Predicting TMCF vulnerability worldwide is the first step
547 to establishing TMCF conservation priorities and prepare human communities for the potential loss of TMCF and the
548 services provided by these ecosystems.

549 **Conflict of Interest**

550 Cleiton B Eller, Leonardo D Meireles, Stephen SO Burgess, Stephen Sitch, Rafael S Oliveira declare that they have
551 no conflict of interest

552 **Human and Animal Rights and Informed Consent**

553 This article does not contain any studies with human or animal subjects performed by any of the authors.

554 **References**

555 1. Bubb P, May I, Miles L, Sayer J. Cloud forest agenda. Cambridge: UNEP-WCMC; 2004.

556 2. Gentry AH. Tropical Forest Biodiversity: Distributional Patterns and Their Conservational Significance. Oikos.
557 1992;63:19–28.

558 • 3. Bruijnzeel LA, Kappelle M, Mulligan M, Scatena FN. Tropical montane cloud forests: State of knowledge and
559 sustainability perspectives in a changing world. Trop Mont Cloud For Sci Conserv Manag. 2011. p. 691–740. **This**
560 **book chapter summarizes very well the advances on cloud forest hydrometeorology and biodiversity research**
561 **up to 2011.**

562 4. Bruijnzeel L. Hydrology of tropical montane cloud forests : A Reassessment. L Use Water Resour Res. 1993;1:1–
563 18.

564 5. Martínez ML, Pérez-Maqueo O, Vázquez G, Castillo-Campos G, García-Franco J, Mehltreter K, et al. Effects of
565 land use change on biodiversity and ecosystem services in tropical montane cloud forests of Mexico. For Ecol
566 Manage. 2009;258:1856–63.

567 6. Stadtmüller T. Cloud forests in the humid tropics: a bibliographic review. Turrialba: CATIE; 1987.

568 7. Bruijnzeel LA, Proctor J. Hydrology and Biogeochemistry of Tropical Montane Cloud Forests: What Do We
569 Really Know? 1995. p. 38–78.

570 8. Grubb PJ. Control of Forest Growth and Distribution on Wet Tropical Mountains: with Special Reference to
571 Mineral Nutrition. Annu Rev Ecol Syst. 1977;

572 • 9. Bertoncello R, Yamamoto K, Meireles LD, Shepherd GJ. A phytogeographic analysis of cloud forests and other
573 forest subtypes amidst the Atlantic forests in south and southeast Brazil. Biodivers Conserv. 2011;20:3413–33. **This**
574 **paper presents a floristic analysis on South/Southeast Brazil Cloud forests showing that they consitute a**
575 **distinct phytogeografic formation from other atlantic forest subtypes.**

576 10. van de Weg MJ, Meir P, Grace J, Atkin OK. Altitudinal variation in leaf mass per unit area, leaf tissue density
577 and foliar nitrogen and phosphorus content along an Amazon-Andes gradient in Peru. Plant Ecol Divers.
578 2009;2:243–54.

579 • 11. Fisher JB, Malhi Y, Torres IC, Metcalfe DB, van de Weg MJ, Meir P, et al. Nutrient limitation in rainforests
580 and cloud forests along a 3,000-m elevation gradient in the Peruvian Andes. Oecologia. 2013;172:889–902. **This**
581 **paper presents the results of a large-scale experiment along an altitudinal transect in the Peruvian Andes. It**
582 **shows higher altitude forests responded to N addition with increased stem diameter growth, but no changes**

in canopy structure and or leaf stoichometry.

12. Falkenberg D, Voltolini JC. The Montane Cloud Forest in Southern Brazil. Trop Mont Cloud For. New York: Springer New York; 1995. p. 138–49.

13. Meireles LD, Shepherd GJ. Structure and floristic similarities of upper montane forests in Serra Fina mountain range, southeastern Brazil. Acta Bot Brasilica. 2015;29:58–72.

14. Merlin MD, Juvik JO. Montane Cloud Forest in the Tropical Pacific: Some Aspects of Their Floristics, Biogeography, Ecology, and Conservation. Trop Mont cloud For. New York: Springer New York; 1995. p. 234–53.

15. Rzedowski J. Analsis preliminar de la flora vascular de los bosques mesofilos de montaña de Mexico. Acta Bot Mex. 1996;35:25–44.

16. Foster P. The potential negative impacts of global climate change on tropical montane cloud forests. Earth-Science Rev [Internet]. 2001;55:73–106. Available from: http://linkinghub.elsevier.com/retrieve/pii/S0012825201000563

17. Leo M. The Importance of Tropical Montane Cloud Forest for Preserving Vertebrate Endemism in Peru: The Río Abiseo National Park as a Case Study. Trop Mont Cloud For. New York: Springer New York; 1995. p. 198–211.

18. Pounds JA, Fogden MPL, Campbell JH. Biological response to climate change on a tropical mountain. Nature. 1999;398:611–5.

19. Still CJ, Foster PN, Schneider SH. Simulating the effects of climate change on tropical montane cloud forests. Nature. 1999;398:608–10.

20. Lawton RO, Nair US, Pielke S, Welch RM. Climatic impact of tropical lowland deforestation on nearby montane cloud forests. Science (80-). 2001;294:584–7.

21. Goldsmith GR, Matzke NJ, Dawson TE. The incidence and implications of clouds for cloud forest plant water relations. Ecol Lett. 2013;16:307–14.

• 22. Oliveira RS, Eller CB, Bittencourt PRL, Mulligan M. The hydroclimatic and ecophysiological basis of cloud forest distributions under current and projected climates. Ann Bot. 2014;113:909–20. **This review paper focuses on the interactions between fog and cloud forest vegetation, especially on the process of direct foliar water uptake and its implications for the vegetation responses to climate change. Besides the ecophysiological framework proposed in the paper, it presents model projections for future cloud forest climate.**

23. Gotsch SG, Nadkarni N, Darby A, Glunk A, Dix M, Davidson K, et al. Life in the treetops: Ecophysiological strategies of canopy epiphytes in a tropical montane cloud forest. Ecol Monogr. 2015;85:393–412.

24. Eller CB, Lima AL, Oliveira RS. Cloud forest trees with higher foliar water uptake capacity and anisohydric

614 behavior are more vulnerable to drought and climate change. New Phytol. 2016;211:489–501.

615 25. Eller CB, Lima AL, Oliveira RS. Foliar uptake of fog water and transport belowground alleviates drought effects
616 in the cloud forest tree species, Drimys brasiliensis (Winteraceae). New Phytol. 2013;199:151–62.

617 26. Eller CB, Burgess SSO, Oliveira RS. Environmental controls in the water use patterns of a tropical cloud forest
618 tree species, Drimys brasiliensis (Winteraceae). Tree Physiol. 2015;35:387–99.

619 27. Pepin N, Bradley RS, Diaz HF, Baraer M, Caceres EB, Forsythe N, et al. Elevation-dependent warming in
620 mountain regions of the world. Nat. Clim. Chang. 2015. p. 424–30.

621 28. Mcgill BJ, Enquist BJ, Weiher E, Westoby M. Rebuilding community ecology from functional traits. 2006;21.

622 29. Sitch S, Huntingford C, Gedney N, Levy PE, Lomas M, Piao SL, et al. Evaluation of the terrestrial carbon cycle,
623 future plant geography and climate-carbon cycle feedbacks using five Dynamic Global Vegetation Models
624 (DGVMs). Glob Chang Biol. 2008;14:2015–39.

625 30. Cox PM, Betts RA, Collins M, Harris PP, Huntingford C, Jones CD. Amazonian forest dieback under climate-
626 carbon cycle projections for the 21st century. Theor Appl Climatol. 2004;78:137–56.

627 31. Bruijnzeel L., Veneklaas E. Climatic conditions and tropical montane forest productivity: The fog has not lifted
628 yet. Ecology. 1998;79:3–9.

629 32. Sperry JS, Venturas MD, Anderegg WRL, Mencuccini M, Mackay DS, Wang Y, et al. Predicting stomatal
630 responses to the environment from the optimization of photosynthetic gain and hydraulic cost. Plant Cell Environ.
631 2017;40:816–30.

632 33. Eller CB, Rowland L, Oliveira RS, Bittencourt PRL, Barros F V., da Costa ACL, et al. Modelling tropical forest
633 responses to drought and El Niño with a stomatal optimization model based on xylem hydraulics. Philos Trans R
634 Soc Lond B Biol Sci. 2018;373:20170315.

635 34. Choat B, Jansen S, Brodribb TJ, Cochard H, Delzon S, Bhaskar R, et al. Global convergence in the vulnerability
636 of forests to drought. Nature. 2012;491:752–5.

637 35. Kattge J, Díaz S, Lavorel S, Prentice IC, Leadley P, Bönisch G, et al. TRY - a global database of plant traits.
638 Glob Chang Biol. 2011;17:2905–35.

639 36. Borcard D, Legendre P, Gillet F. Numerical Ecology with R: Use R! Springer. 2011.

640 37. Reich PB. The world-wide "fast-slow" plant economics spectrum: A traits manifesto. J Ecol. 2014;102:275–301.

641 38. Buckley RC, Corlett RT, Grubb PJ. Are the Xeromorphic Trees of Tropical Upper Montane Rain Forests
642 Drought- Resistant? Biotropica. 1980;12:124–36.

643 • 39. Jarvis A, Mulligan M. The climate of cloud forests. Array, editor. Hydrol Process [Internet]. John Wiley &

644 Sons, Ltd.; 2011 [cited 2013 Jan 27];25:327–43. Available from: http://doi.wiley.com/10.1002/hyp.7847 **This paper**
645 **provides a very useful description of the climate of cloud forest thoughout the planet. Showing that cloud**
646 **forests are significantly colder and more humid than other montane forests not affected by clouds.**

647 40. Gale J. Elevation and Transpiration: Some Theoretical Considerations with Special Reference to Mediterranean-
648 Type Climate. J Appl Ecol. 1972;9:691–702.

649 41. Smith WK, Geller GN. Plant transpiration at high elevations: Theory, field measurements, and comparisons with
650 desert plants. Oecologia. 1979;41:109–22.

651 42. Leuschner C. Are High Elevations in Tropical Mountains Arid Environments for Plants ? Ecology.
652 2000;81:1425–36.

653 43. Tanner EVJ, Vltousek PM, Cuevas E. Experimental investigation of nutrient limitation of forest growth on wet
654 tropical mountains. Ecology. 1998;79:10–22.

655 44. Kitayama K, Aiba SI. Ecosystem structure and productivity of tropical rain forests along altitudinal gradients
656 with contrasting soil phosphorus pools on Mount Kinabalu,Borneo. J Ecol. 2002;90:37–51.

657 45. Soethe N, Lehmann J, Engels C. Nutrient availability at different altitudes in a tropical montane forest in
658 Ecuador. J Trop Ecol. 2008;24:397–406.

659 46. Weaver PL, Medina E, Pool D, Dugger K, Gonzales-Liboy J, Cuevas E. Ecological Observations in the Dwarf
660 Cloud Forest of the Luquillo Mountains in Puerto Rico. Biotropica. 1986;18:79–85.

661 47. Wright IJ, Reich PB, Westoby M, Ackerly DD, Baruch Z, Bongers F, et al. The worldwide leaf economics
662 spectrum. 2004;12:821–7.

663 48. Poorter H, Niinemets Ü, Poorter L, Wright IJ, Villar R. Causes and consequences of variation in leaf mass per
664 area (LMA): a meta-analysis. 2009;565–88.

665 49. Grieve B. Negative turgor pressures in sclerophyll plants. Aust J Sci. 1961;23:375–7.

666 50. Zhu SD, Chen YJ, Ye Q, He PC, Liu H, Li RH, et al. Leaf turgor loss point is correlated with drought tolerance
667 and leaf carbon economics traits. Tree Physiol. 2018;38:658–63.

668 51. Jane GT, Green TGA. Patterns of Stomatal Conductance in Six Evergreen Tree Species from a New Zealand
669 Cloud Forest. Bot Gaz. 1986;146:413–20.

670 52. Cavelier J. Tissue water relations in elfin cloud forest tree species of Serrania de Macuira, Guajira, Colombia.
671 Trees. 1990;4:155–63.

672 53. Gotsch SG, Crausbay SD, Giambelluca TW, Weintraub AE, Longman RJ, Asbjornsen H, et al. Water relations
673 and microclimate around the upper limit of a cloud forest in Maui, Hawai'i. Tree Physiol. 2014;34:766–77.

674 54. Maréchaux I, Bartlett MK, Sack L, Baraloto C, Engel J, Joetzjer E, et al. Drought tolerance as predicted by leaf
675 water potential at turgor loss point varies strongly across species within an Amazonian forest. Funct Ecol.
676 2015;29:1268–77.

677 55. Yamori W, Hikosaka K, Way DA. Temperature response of photosynthesis in C3, C4, and CAM plants:
678 Temperature acclimation and temperature adaptation. Photosynth Res. 2014;119:101–17.

679 56. Letts MG, Mulligan M. The impact of light quality and leaf wetness on photosynthesis in north-west Andean
680 tropical montane cloud forest. J Trop Ecol. 2005;21:549–57.

681 57. van de Weg MJ, Meir P, Grace J, Ramos GD. Photosynthetic parameters, dark respiration and leaf traits in the
682 canopy of a Peruvian tropical montane cloud forest. Oecologia. 2012;168:23–34.

683 58. Wittich B, Horna V, Homeier J, Leuschner C. Altitudinal Change in the Photosynthetic Capacity of Tropical
684 Trees: A Case Study from Ecuador and a Pantropical Literature Analysis. Ecosystems. 2012;15:958–73.

685 59. Güsewell S. N:P ratios in terrestrial plants: Variation and functional significance. New Phytol. 2004;164:243–66.

686 60. Aerts R, Chapin FS. The Mineral Nutrition of Wild Plants Revisited: A Re-evaluation of Processes and Patterns.
687 Adv Ecol Res. 1999;30:1–67.

688 61. Gerrish G, Mueller-Dombois D, Bridges KW. Nutrient limitation and Metrosideros forest dieback in Hawaii.
689 Ecology. 1988;69:723–7.

690 62. Raich JW, Russell AE, Crews TE, Farrington H, Vitousek PM. Both nitrogen and phosphorus limit plant
691 production on young Hawaiian lava flows. Biogeochemistry. 1996;32:1–14.

692 • 63. Fahey TJ, Sherman RE, Tanner EVJ. Tropical montane cloud forest: Environmental drivers of vegetation
693 structure and ecosystem function. J Trop Ecol. 2016;32:355–67. **This review explores how environmental**
694 **conditions in cloud forests might cause its particular morphology and low productivity. The authors propose**
695 **cloud immersion as the main driver of soil nutrient limitation and vegetation functioning.**

696 64. Güsewell S, Koerselman W. Variation in nitrogen and phosphorus concentrations of wetland plants. Perspect
697 Plant Ecol Evol Syst. 2002;5:37–61.

698 65. Berry ZC, White JC, Smith WK. Foliar uptake, carbon fluxes and water status are affected by the timing of daily
699 fog in saplings from a threatened cloud forest. Tree Physiol. 2014;34:459–70.

700 66. Burkhardt J, Basi S, Pariyar S, Hunsche M. Stomatal penetration by aqueous solutions - an update involving leaf
701 surface particles. New Phytol. 2012;196:774–87.

702 67. Boanares D, Isaias RRMS, de Sousa HC, Kozovits AR. Strategies of leaf water uptake based on anatomical
703 traits. Plant Biol. 2018;20:848–56.

704 68. Benzing DH, Burt KM. Foliar Permeability Among Twenty Species of the Bromeliaceae. Bull Torrey Bot Club.

1970;97:269.

69. Berry ZC, Emery NC, Gotsch SG, Goldsmith GR. Foliar water uptake: Processes, pathways, and integration into plant water budgets. Plant Cell Environ. 2019;42:410–23.

70. Binks O, Mencuccini M, Rowland L, da Costa ACL, de Carvalho CJR, Bittencourt P, et al. Foliar water uptake in Amazonian trees: Evidence and consequences. Glob Chang Biol. 2019;25:2678–90.

71. Dawson TE, Goldsmith GR. The value of wet leaves. New Phytol. 2018;219:1156–69.

72. Arriaga L. Types and causes of tree mortality in a tropical montane cloud forest of Tamaulipas, Mexico. J Trop Ecol. 2000;16:623–36.

73. Soethe N, Lehmann J, Engels C. Root morphology and anchorage of six native tree species from a tropical montane forest and an elfin forest in Ecuador. Plant Soil. 2006;279:173–85.

74. Werner WL. Canopy dieback in the upper montane rain forests of Sri Lanka. GeoJournal. 1988;17:245–8.

75. Lowry JB, Lee DW, Stone. BC. Effects of drought on Mount Kinabalu. Malayan Nat J. 1973;26:178–1799.

76. Hutley LB, Doley D, Yates DJ, Boonsaner A. Water balance of an australian subtropical rainforest at altitude: The ecological and physiological significance of intercepted cloud and fog. Aust J Bot. 1997;45:311–29.

77. Cavelier J, Goldstein G. Mist and fog interception in elfin cloud forests in Colombia and Venezuela. J Trop Ecol. 1989;5:309–22.

78. Holder CD. Rainfall interception and fog precipitation in a tropical montane cloud forest of Guatemala. For Ecol Manage. 2004;190:373–84.

79. Benzing DH. Vulnerabilities of tropical forests to climate change: The significance of resident epiphytes. Clim Change. 1998. p. 519–40.

80. Adriaenssens S, Staelens J, Wuyts K, De Schrijver A, Van Wittenberghe S, Wuytack T, et al. Foliar nitrogen uptake from wet deposition and the relation with leaf wettability and water storage capacity. Water Air Soil Pollut. 2011;219:43–57.

81. Weathers KC, Lovett GM, Likens GE, Caraco NFM. Cloudwater inputs of nitrogen to forest ecosystem in southern Chile: Forms, fluxes, and sources. Ecosystems. 2000;3:590–5.

82. Matson AL, Corre MD, Burneo JI, Veldkamp E. Free-living nitrogen fixation responds to elevated nutrient inputs in tropical montane forest floor and canopy soils of southern Ecuador. Biogeochemistry. 2015;122:281–94.

83. Benner JW, Conroy S, Lunch CK, Toyoda N, Vitousek PM. Phosphorus fertilization increases the abundance and nitrogenase activity of the cyanolichen Pseudocyphellaria crocata in Hawaiian montane forests. Biotropica. 2007;39:400–5.

735 84. Mencuccini M, Manzoni S, Christoffersen B. Modelling water fluxes in plants: from tissues to biosphere. New
736 Phytol. 2019;222:1207–22.

737 85. Brodribb TJ, Cochard H. Hydraulic Failure Defines the Recovery and Point of Death in Water-Stressed
738 Conifers. Plant Physiol. 2009;149:575–84.

739 86. Maherali H, Pockman WT, Jackson RB. Adaptive variation in the vulnerability of woody plants to xylem
740 cavitation. Ecology. 2004;85:2184–99.

741 87. Oliveira RS, Costa FRC, van Baalen E, de Jonge A, Bittencourt PR, Almanza Y, et al. Embolism resistance
742 drives the distribution of Amazonian rainforest tree species along hydro-topographic gradients. New Phytol.
743 2019;221:1457–65.

744 88. Eller CB, de V. Barros F, R.L. Bittencourt P, Rowland L, Mencuccini M, S. Oliveira R. Xylem hydraulic safety
745 and construction costs determine tropical tree growth. Plant Cell Environ. 2018;41:548–62.

746 89. Hacke UG, Sperry JS, Feild TS, Sano Y, Sikkema EH, Pittermann J. Water Transport in Vesselless
747 Angiosperms: Conducting Efficiency and Cavitation Safety. Int J Plant Sci. 2007;168:1113–26.

748 90. Sperry JS, Hacke UG, Feild TS, Sano Y, Sikkema EH. Hydraulic Consequences of Vessel Evolution in
749 Angiosperms. Int J Plant Sci. 2007;168:1127–39.

750 91. Christoffersen BO, Gloor M, Fauset S, Fyllas NM, Galbraith DR, Baker TR, et al. Linking hydraulic traits to
751 tropical forest function in a size-structured and trait-driven model (TFS v.1-Hydro). Geosci Model Dev.
752 2016;9:4227–55.

753 92. Meinzer FC, Johnson DM, Lachenbruch B, McCulloh KA, Woodruff DR. Xylem hydraulic safety margins in
754 woody plants: Coordination of stomatal control of xylem tension with hydraulic capacitance. Funct Ecol.
755 2009;23:922–30.

756 93. Zotz G, Tyree MT, Patiño S, Carlton MR. Hydraulic architecture and water use of selected species from a lower
757 montane forest in Panama. Trees - Struct Funct. 1998;12:302–9.

758 94. Feild TS, Holbrook NM. Xylem sap flow and stem hydraulics of the vesselles angiosperm Drimys granadensis
759 (Winteraceae) in a Costa Rican elfin forest. Plant, Cell Environ. 2000;23:1067–77.

760 95. Sperry JS, Hacke UG, Pittermann J. Size and function in conifer tracheids and angiosperm vessels. Am J Bot.
761 2006;93:1490–500.

762 96. Davis SD, Sperry JS, Hacke UG. The relationship between xylem conduit diameter and cavitation caused by
763 freezing. Am J Bot. 1999;86:1367–72.

764 97. Rehm EM, Feeley KJ, Meinzer FC. Freezing temperatures as a limit to forest recruitment above tropical Andean
765 treelines. Ecology. 2015;96:1856–65.

766 98. Santiago LS, Jones TJ, Goldstein G. Physiological variation in Hawaiian metrosideros polymorpha across a
767 range of habitats: From dry forests to cloud forests. Trop Mont Cloud For Sci Conserv Manag. 2011. p. 456–64.

768 99. McDowell N, Barnard H, Bond BJ, Hinckley T, Hubbard RM, Ishii H, et al. The relationship between tree height
769 and leaf area: Sapwood area ratio. Oecologia. 2002;132:12–20.

770 100. Ryan MG, Yoder BJ. Hydraulic Limits to Tree Height and Tree Growth. Bioscience. 2006;47:235–42.

771 101. Jaffe MJ. Thigmomorphogenesis: The response of plant growth and development to mechanical stimulation.
772 Planta. 1973;114:143–57.

773 102. Lawton RO. Wind stress and elfin stature in a montane rain forest tree: an adaptive explanation. Am J Bot.
774 1982;69:1224–30.

775 103. Lawton RO. Ecological constraints on wood density in a tropical montane rain forest. Am J Bot. 1984;71:261–
776 7.

777 104. King DA, Aug N. Tree form, height growth, and susceptibility to wind damage in Acer saccharum. Ecology.
778 1986;67:980–90.

779 105. Curran TJ, Gersbach LN, Edwards W, Krockenberger AK. Wood density predicts plant damage and vegetative
780 recovery rates caused by cyclone disturbance in tropical rainforest tree species of North Queensland, Australia.
781 Austral Ecol. 2008;33:442–50.

782 106. Chave J, Muller-Landau HC, Baker TR, Easdale TA, Hans Steege TER, Webb CO. Regional and phylogenetic
783 variation of wood density across 2456 neotropical tree species. Ecol Appl. 2006;16:2356–67.

784 107. Leuschner C, Moser G, Bertsch C, Röderstein M, Hertel D. Large altitudinal increase in tree root/shoot ratio in
785 tropical mountain forests of Ecuador. Basic Appl Ecol. 2007;8:219–30.

786 108. Girardin CAJ, Malhi Y, Aragão LEOC, Mamani M, Huaraca Huasco W, Durand L, et al. Net primary
787 productivity allocation and cycling of carbon along a tropical forest elevational transect in the Peruvian Andes. Glob
788 Chang Biol. 2010;16:3176–92.

789 109. Moser G, Leuschner C, Hertel D, Graefe S, Soethe N, Iost S. Elevation effects on the carbon budget of tropical
790 mountain forests (S Ecuador): The role of the belowground compartment. Glob Chang Biol. 2011;

791 110. Bloom AJ, Chapin FS, Mooney HA. Resource Limitation in Plants-An Economic Analogy. Annu Rev Ecol
792 Syst. 1985;16:363–92.

793 111. Ericsson T. Growth and shoot: root ratio of seedlings in relation to nutrient availability. Plant Soil. 1995;168–
794 169:205–14.

795 112. Girardin CAJ, Aragão LEOC, Malhi Y, Huaraca Huasco W, Metcalfe DB, Durand L, et al. Fine root dynamics
796 along an elevational gradient in tropical Amazonian and Andean forests. Global Biogeochem Cycles. 2013;27:252–

64.

113. Metcalfe DB, Meir P, Aragão LEOC, Da Costa ACL, Braga AP, Gonçalves PHL, et al. The effects of water availability on root growth and morphology in an Amazon rainforest. Plant Soil. 2008;311:189–99.

114. Clark LJ, Whalley WR, Barraclough PB. How do roots penetrate strong soil? Plant Soil. 2003;255:93–104.

115. Huber DPW, Philippe RN, Madilao LL, Sturrock RN, Bohlmann J. Changes in anatomy and terpene chemistry in roots of Douglas-fir seedlings following treatment with methyl jasmonate. Tree Physiol. 2005;25:1075–83.

116. Engels C, Marschner H. Effect of sub-optimal root zone temperatures at varied nutrient supply and shoot meristem temperature on growth and nutrient concentrations in maize seedlings (Zea mays L.). Plant Soil. 1990;126:215–25.

117. Bigot J, Boucaud J. Short-term responses of Brassica rapa plants to low root temperature: Effects on nitrate uptake and its translocation to the shoot. Physiol Plant. 1996;96:646–54.

118. Köhler L, Tobón C, Frumau KFA, Bruijnzeel LA. Biomass and water storage dynamics of epiphytes in old-growth and secondary montane cloud forest stands in Costa Rica. Plant Ecol. 2007;193:171–84.

119. Hofstede RGM, Wolf JHD. Epiphytic biomass and nutrient status of a Colombian upper montane rain forest. Biomasa de epífitas y estado nutricional de un bosque lluvioso colombiano de altura. Selbyana. 1993;14:37–45.

120. Collatz GJ, Ball JT, Grivet C, Berry JA. Physiological and environmental regulation of stomatal conductance, photosynthesis and transpiration: a model that includes a laminar boundary layer. Agric For Meteorol. 1991;54:107–36.

121. Kattge J, Knorr W, Raddatz T, Wirth C. Quantifying photosynthetic capacity and its relationship to leaf nitrogen content for global-scale terrestrial biosphere models. Glob Chang Biol. 2009;15:976–91.

122. Harper AB, Cox PM, Friedlingstein P, Wiltshire AJ, Jones CD, Sitch S, et al. Improved representation of plant functional types and physiology in the Joint UK Land Environment Simulator (JULES v4.2) using plant trait information. Geosci Model Dev. 2016;9:2415–40.

123. Carswell FE, Meir P, Wandelli E V., Bonates LCM, Kruijt B, Barbosa EM, et al. Photosynthetic capacity in a central Amazonian rain forest. Tree Physiol [Internet]. 2000;20:179–86. Available from: https://academic.oup.com/treephys/article-lookup/doi/10.1093/treephys/20.3.179

124. Domingues TF, Martinelli LA, Ehleringer JR. Ecophysiological traits of plant functional groups in forest and pasture ecosystems from eastern Amazônia, Brazil. Plant Ecol. 2007;193:101–12.

125. Coste S, Roggy JC, Imbert P, Born C, Bonal D, Dreyer E. Leaf photosynthetic traits of 14 tropical rain forest species in relation to leaf nitrogen concentration and shade tolerance. Tree Physiol. 2005;25:1127–37.

126. Bittencourt PRL, Barros F de V., Eller CB, Müller CS, Oliveira RS. The fog regime in a tropical montane cloud

forest in Brazil and its effects on water, light and microclimate. Agric For Meteorol. 2019;265:359–69.

127. Smith WK, McClean TM. Adaptive Relationship Between Leaf Water Repellency, Stomatal Distribution, and Gas Exchange. Am J Bot. 2006;76:465–9.

128. Clark DB, Mercado LM, Sitch S, Jones CD, Gedney N, Best MJ, et al. The Joint UK Land Environment Simulator (JULES), Model description – Part 2: Carbon fluxes and vegetation. Geosci Model Dev Discuss [Internet]. 2011;4:641–88. Available from: http://www.geosci-model-dev-discuss.net/4/641/2011/

129. Kattge J, Knorr W. Temperature acclimation in a biochemical model of photosynthesis: A reanalysis of data from 36 species. Plant, Cell Environ. 2007;30:1176–90.

130. Mercado LM, Medlyn BE, Huntingford C, Oliver RJ, Clark DB, Sitch S, et al. Large sensitivity in land carbon storage due to geographical and temporal variation in the thermal response of photosynthetic capacity. New Phytol. 2018;218:1462–77.

131. Adams WW, Cohu CM, Muller O, Demmig-Adams B. Foliar phloem infrastructure in support of photosynthesis. Front Plant Sci. 2013;4.

132. Wardlaw IF, Bagnall D. Phloem Transport and the Regulation of Growth of Sorghum bicolor (Moench) at Low Temperature. Plant Physiol. 1981;68:411–4.

133. Cavender-Bares J. Impacts of Freezing on Long Distance Transport in Woody Plants. Vasc Transp Plants. 2005. p. 401–24.

134. Körner C. Paradigm shift in plant growth control. Curr Opin Plant Biol. 2015;25:107–14.

135. Rosado BHP, Joly CA, Burgess SSO, Oliveira RS, Aidar MPM. Changes in plant functional traits and water use in Atlantic rainforest: evidence of conservative water use in spatio-temporal scales. Trees - Struct Funct. 2016;30:47–61.

136. Rada F, García-Núñez C, Ataroff M. Leaf Gas Exchange in Canopy Species of a Venezuelan Cloud Forest. Biotropica. 2009;41:659–64.

137. Feild TS, Zwieniecki MA, Donoghue MJ, Holbrook NM. Stomatal plugs of Drimys winteri (Winteraceae) protect leaves from mist but not drought. Proc Natl Acad Sci. 2002;95:14256–9.

138. Diaz S, Cabido M, Casanoves F. Plant functional traits and environmental filters at a regional scale. J Veg Sci [Internet]. 1998;9:113–22. Available from: http://doi.wiley.com/10.2307/3237229

139. Salinas N, Malhi Y, Meir P, Silman M, Roman Cuesta R, Huaman J, et al. The sensitivity of tropical leaf litter decomposition to temperature: Results from a large-scale leaf translocation experiment along an elevation gradient in Peruvian forests. New Phytol. 2011;189:967–77.

140. Toome M, Heinsoo K, Luik A. Relation between leaf rust (Melampsora epitea) severity and the specific leaf

area in short rotation coppice willows. Eur J Plant Pathol. 2010;126:583–8.

141. Poorter L. Leaf traits show different relationships with shade tolerance in moist versus dry tropical forests. New Phytol. 2009;

142. De Kauwe MG, Medlyn BE, Pitman AJ, Drake JE, Ukkola A, Griebel A, et al. Examining the evidence for decoupling between photosynthesis and transpiration during heat extremes. Biogeosciences. 2019;16:903–16.

143. Cordero RA. Ecophysiology of Cecropia schreberiana saplings in two wind regimes in an elfin cloud forest: Growth, gas exchange, architecture and stem biomechanics. Tree Physiol. 1999;19:153–63.

144. Gardiner B, Berry P, Moulia B. Review: Wind impacts on plant growth, mechanics and damage. Plant Sci. 2016. p. 94–118.

145. Van Gelder HA, Poorter L, Sterck FJ. Wood mechanics, allometry, and life-history variation in a tropical rain forest tree community. New Phytol. 2006;171:367–78.

146. Hildebrandt A, Eltahir EAB. Ecohydrology of a seasonal cloud forest in Dhofar: 2. Role of clouds, soil type, and rooting depth in tree-grass competition. Water Resour Res. 2007;43.

147. Kraft NJB, Adler PB, Godoy O, James EC, Fuller S, Levine JM. Community assembly, coexistence and the environmental filtering metaphor. Funct Ecol. 2015;29:592–9.

148. Spracklen D V., Righelato R. Tropical montane forests are a larger than expected global carbon store. Biogeosciences. 2014;11:2741–54.

149. Suhs RB, Hoeltgebaum MP, Nuernberg-Silva A, Fiaschi P, Neckel-Oliveira S, Peroni N. Species diversity, community structure and ecological traits of trees in an upper montane forest, southern Brazil. Acta Bot Brasilica. 2019;33:153–62.

150. Koehler A, Galvão F, Longhi SJ. Floresta Ombrófila Densa Altomontana: aspectos florísticos e estruturais de diferentes trechos na Serra do Mar, PR. Ciência Florest. 2005;12:27.

151. Valente ASM, Garcia PO, Salimena FRG, De Oliveira-Filho AT. Composição, estrutura e similaridade florística da Floresta Atlântica, na Serra Negra, Rio Preto - MG. Rodriguesia. 2011;62:321–40.

152. Costa M do P, Pereira JAA, Fontes MAL, de Melo PHA, Pífano DS, Pellicciottii AS, et al. Estrutura e diversidade da comunidade arbórea de uma floresta superomontana, no planalto de Poços de Caldas (MG). Cienc Florest. 2011;21:711–25.

153. Colonetti S, Citadini-Zanette V, Martins R, dos Santos R, Rocha E, Jarenkow JA. Florística e estrutura fitossociológica em floresta ombrófila densa submontana na barragem do rio São Bento, Siderópolis, Estado de Santa Catarina. Acta Sci - Biol Sci. 2009;31:397–405.

154. Silva FC da. Composição florística e estrutura fitossociológica da floresta tropical ombrófila da encosta

890 Atlântica no município de Morretes, Estado do Paraná. Acta Biológica Parana. 1994;23:1–54.

891 155. Guilherme FAG, Morellato LPC, Assis MA. Horizontal and vertical tree community structure in a lowland
892 atlantic rain forest, southeastern Brazil. Rev Bras Botânica. 2004;27:725–37.

893 156. Dias AC, Couto HTZ Do. Comparação De Métodos De Amostragem Na Floresta Ombrófila Densa – Parque
894 Estadual Carlos Botelho/Sp–Brasil. Rev.Inst.Flor., São Paulo. 2005.

895 157. Rochelle ALC, Cielo-Filho R, Martins FR. Tree community structure in an Atlantic forest fragment at Serra do
896 Mar State Park, southeastern Brazil. Biota Neotrop. 2011;11:337–46.

897 158. Carvalho WAC, Filho ARYTO, Fontes MAL. Variação espacial da estrutura da comunidade arbórea de um
898 fragmento de floresta semidecídua em Piedade do Rio Grande , MG , Brasil. 2007;315–35.

899 159. Prata EMB, Assis MA, Joly CA. Floristic composition and structure of tree community on the transition
900 Lowland - Lowermontane Ombrophilous Dense Forest in N?cleo Picinguaba/Serra do Mar State Park, Ubatuba,
901 southeastern Brazil. Biota Neotrop. 2011;11:285–99.

902 **Figure legends**

903 **Figure 1.** Biplot of a Principal Component Analysis (PCA) and altitudinal trends of the community averaged
904 functional traits from the South/Southeast Brazil sites. In the PCA biplot in the left, the arrows show the five functional
905 traits most strongly associated with the first two PCA components (HV: Huber value, K_s: Sapwood specific
906 conductivity, SLA: Specific leaf area, N_m: Leaf nitrogen on a mass basis, ρ: Sapwood density). The red and blue
907 clusters were defined using a *k*-means clustering algorithm based on the data silhouette width. In the panels on the
908 right, the sites in blue are Tropical Montane Cloud Forests and the sites in red are other types of Atlantic forests (see
909 Table 1). The meaning of the functional traits' acronyms is given in Table 2. We only used the sites from Table 1
910 where we could find genus-level trait data enough to cover at least 50 % of the community total stem basal area.

911 **Figure 2.** Rubisco maximum carboxylation rate (V_{cmax}) responses to leaf temperature (T_l) in Tropical Montane Cloud
912 Forest (CF) and non-CF species (a). The continuous lines is the response of non-acclimated species, that is, the T_{low}
913 and T_{upp} parameters from equation 2 are assumed to be equal to the parameters used in Harper et al [122]. In the dotted
914 lines the equations from Kattge & Knorr [129] were used to simulate plant acclimation to the observed mean annual
915 temperature at the sites (95% confidence interval for CF and non-CF sites represented as the blue and red shaded
916 regions, respectively). In (b) to (d) we show the predicted altitudinal trend of each of the limiting steps in the process
917 of photosynthesis (A_n) according with Collatz et al [120]. The yellow line is the light-limited rate (J_l), the green line
918 is the Rubisco carboxylation limited rate (J_c) and the grey line is the transport limited rate (J_e). The J_l rate was
919 computed to represent low radiation conditions (Incident photosynthetic active radiation of 180 μmol m^{-2} s^{-1}). The
920 continuous lines assume no thermal acclimation of V_{cmax}, and the dotted lines are the acclimated responses. In panel
921 (b), only the atmospheric pressure (p_a), and consequently the partial pressure of CO_2 (c_a) and O_2 declines with altitude.
922 In (b), only air temperature (T_a) declines with altitude. In (c) all variables change with altitude. The leaf internal CO_2
923 partial pressure in the model was assumed to be 0.7 of the c_a and leaf temperature was assumed equal to air temperature.

The model V_{cmax} was computed based on the observed leaf N and SLA for TMCF (see details in text), and the other photosynthetic parameters were set equal to Harper et al [122]. On the right we show the modelled **s**tomatal conductance (g_s; e-f) and leaf water potential (Ψ; g-h) responses to leaf to air vapor pressure deficit (D) and root Ψ. The blue lines represent CF trees, and the red lines non-CF trees. The dashed lines represent the environmental conditions at 2250 m and the continuous lines are the environmental conditions at sea-level. The hydraulic and photosynthetic parameters used in the model are derived from Fig. 1. The differences in temperature between seal level and 2250 were based on the lapse rate from Fig. S2, and altitudinal changes in the incident shortwave radiation were modelled following Leuschner [42]. The mean wind speed was constant at 2 m s^{-1}. In the panels (e-g) the root Ψ was constant at -0.1 MPa and relative humidity changed from 1 to 95%. In the panels (f-h) the relative humidity was constant at 80% and root Ψ changed from -0.1 to -3 MPa. The full model description is given in Appendix S2.

Figure 3. Huber Value (HV) necessary to sustain a stomatal conductance of 1 mol m^{-2} s^{-1} plotted in function of tree height. The blue lines represent Cloud Forests (CF) trees, and the blue lines represent non-CF trees. The dashed lines represent the environmental conditions at 2250 m. The differences in temperature between seal level and 2250 were based on the lapse rate from Fig. 2, and altitudinal changes in the incident shortwave radiation were modelled following Leuschner [42]. The red and blue shaded regions in the plot are the 95% confidence intervals of the mean tree height observed in CF and non-CF, respectively.

Figure 4. Schematic representation of the relationships between low temperatures and clouds on the Cloud Forest (CF) defining functional traits. The functional traits in blue boxes can be linked to low temperatures, while traits in gray boxes can be linked to cloud immersion.

Tables

Table 1. Cloud forest and non-cloud affected Atlantic forest sites in South/Southeast Brazil. Sites are classified as Cloud Forests (CF) or Atlantic forests not affected by clouds (nCF) based on its source study.

Code	Coordinates	Altitude	Source
CF1	28°08' S 49°28' W	1590 m	Suhs *et al.* [149]
CF2	25°54' S 48°56' W	1610 m	Koehler *et al.* [150]
CF3	25°41' S 49°02' W	1390 m	Koehler *et al* .[150]
CF4	25°32' S 48°56' W	1545 m	Koehler *et al.* [150]
CF5	25°32' S 48°56' W	1460 m	Koehler *et al.* [150]
CF6	25°21' S 48°54' W	1590 m	Koehler *et al.* [150]
CF7	22°41' S 45°25' W	2000 m	Oliveira *et al. unpublished*
CF8	22°26' S 44°51' W	2250 m	Meireles & Shepherd [13]
CF9	21°58' S 43°52' W	1300 m	Valente *et al.* [151]
CF10	21°46' S 46'24' W	1387 m	Costa *et al.* [152]
nCF1	21°59' S 43°53' W	1000 m	Valente *et al.* [151]

nCF2	28°36’ S 49°33’ W	178 m	Colonetti *et al.* [153]
nCF3	25°30’ S 48°38’ W	485 m	Silva [154]
nCF4	24°14’ S 48°04’ W	108 m	Guilherme *et al.* [155]
nCF5	24°00’ S 47°55’ W	650 m	Dias & Couto [156]
nCF6	23°21’ S 45°05’ W	371 m	Rochelle *et al.* [157]
nCF7	22°40’ S 42°30’ W	150 m	Carvalho *et al.* [158]
nCF8	23°20’ S 44°50’ W	55 m	Prata *et al.* [159]

Table 2. Description of traits evaluated at the cloud forest sites in South/Southeast Brazil and measurements of the trait phylogenetic signal with the Pagel’s λ. When Pagel’s λ=0 there is no phylogenetic signal, that is, the trait evolved independently of phylogeny; when λ=1 the trait evolution followed a pure Brownian model of evolution.

Trait	Units	Description	λ	*p*
SLA	$m^2\ kg^{-1}$	Specific leaf area	0.33	<0.01
N_m	$mg\ g^{-1}$	Nitrogen content on a leaf mass basis	0.71	<0.01
A_n	$\mu mol\ m^{-2}\ s^{-1}$	Leaf net carbon assimilation rate	0.12	0.03
Ψ_{50}	MPa	Xylem/Tracheid water potential when plant loses 50% of its maximum hydraulic conductivity	0.51	<0.01
Ψ_{min}	MPa	Minimum leaf water potential at the field	0.21	0.07
π_{tlp}	MPa	Leaf turgor loss point	<0.01	1
K_s	$kg\ m^{-1}\ s^{-1}\ MPa^{-1}$	Xylem/Tracheid specific conductivity	0.1	0.06
HV	$cm^2\ m^{-2}$	Huber Value, the ratio between sapwood area and leaf area	<0.01	1
H_{max}	m	Maximum canopy height	0.75	<0.01
ρ	$g\ cm^{-3}$	Basic wood density	0.42	<0.01

Figures for "*How climate shapes the functioning of Tropical Montane Cloud Forests*"

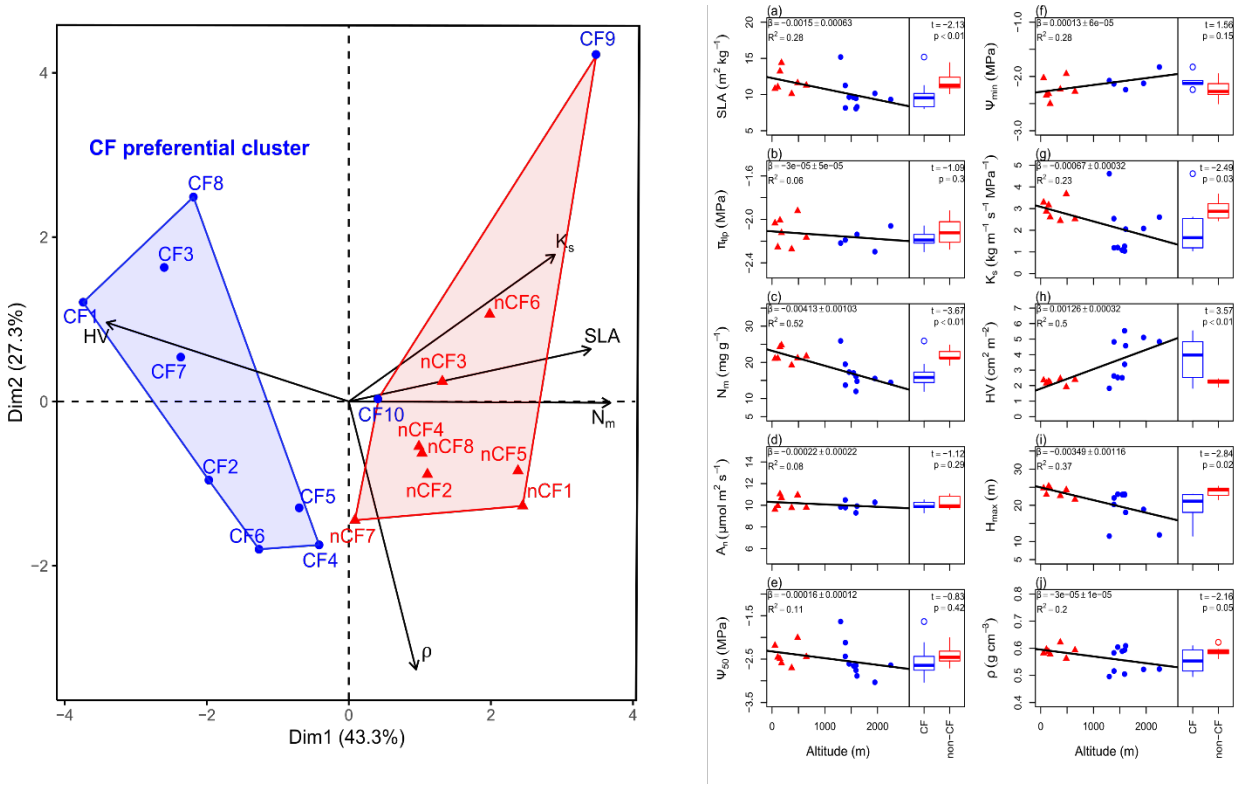

Figure 1. Biplot of a Principal Component Analysis (PCA) and altitudinal trends of the community averaged functional traits from the South/Southeast Brazil sites. In the PCA biplot in the left, the arrows show the five functional traits most strongly associated with the first two PCA components (HV: Huber value, K_s: Sapwood specific conductivity, SLA: Specific leaf area, N_m: Leaf nitrogen on a mass basis, ρ: Sapwood density). The red and blue clusters were defined using a k-means clustering algorithm based on the data silhouette width. In the panels on the right, the sites in blue are Tropical Montane Cloud Forests and the sites in red are other types of Atlantic forests (see Table 1). The meaning of the functional traits' acronyms can be found in Table 2. We only used the sites from Table 1 where we could find genus-level trait data enough to cover at least 50 % of the community total dominance.

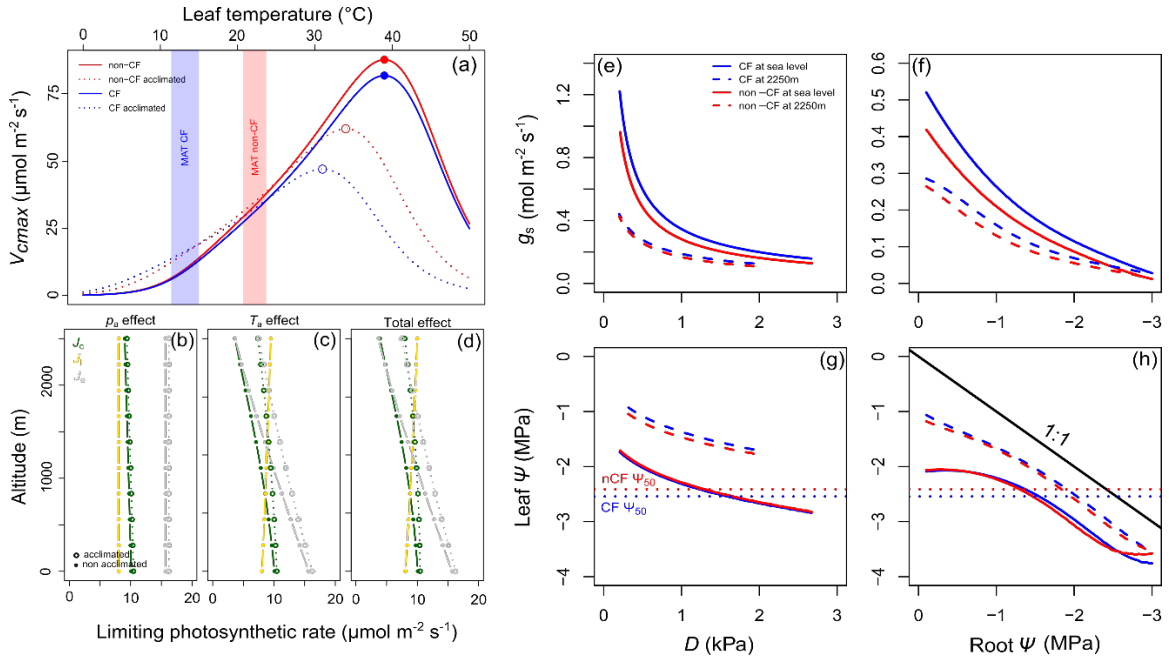

Figure 2. Rubisco maximum carboxylation rate (V_{cmax}) responses to leaf temperature (T_l) in Tropical Montane Cloud Forest (CF) and non-CF species (a). The continuous lines is the response of non-acclimated species, that is, the T_{low} and T_{upp} parameters from equation 2 are assumed to be equal to the parameters used in Harper et al [67]. In the dotted lines the equations from Kattge & Knorr [80] were used to simulate plant acclimation to the observed mean annual temperature at the sites (95% confidence interval for CF and non-CF sites represented as the blue and red shaded regions, respectively). In (b) to (d) we show the predicted altitudinal trend of each of the limiting steps in the process of photosynthesis (A_n) according with Collatz et al [76]. The yellow line is the light-limited rate (J_l), the green line is the Rubisco carboxylation limited rate (J_c) and the grey line is the transport limited rate (J_e). The J_l rate was computed to represent low radiation conditions (Incident photosynthetic active radiation of 180 µmol m^{-2} s^{-1}). The continuous lines assume no thermal acclimation of V_{cmax}, and the dotted lines are the acclimated responses. In panel (b), only the atmospheric pressure (p_a), and consequently the partial pressure of CO_2 (c_a) and O_2 declines with altitude. In (b), only air temperature (T_a) declines with altitude. In (c) all variables change with altitude. The leaf internal CO_2 partial pressure in the model was assumed to be 0.7 of the c_a and leaf temperature was assumed equal to air temperature. The model V_{cmax} was computed based on the observed leaf N and SLA for TMCF (see details in text), and the other photosynthetic parameters were set equal to Harper et al [67]. On the right we show the modelled stomatal conductance (g_s; e-f) and leaf water potential (Ψ; g-h) responses to leaf to air vapor pressure deficit (D) and root Ψ. The blue lines represent CF trees, and the red lines non-CF trees. The dashed lines represent the environmental conditions at 2250 m and the continuous lines are the environmental conditions at sea-level. The hydraulic and photosynthetic parameters used in the model are derived from Fig. 1. The differences in temperature between seal level and 2250 were based on the lapse rate from Fig. S2, and altitudinal changes in the incident shortwave radiation were modelled following Leuschner [42]. The mean wind speed was constant at 2 m s^{-1}. In the panels (e-g) the root Ψ was constant at -0.1 MPa and relative humidity changed from 1 to 95%. In the panels (f-h) the relative humidity was constant at 80% and root Ψ changed from -0.1 to -3 MPa. The full model description is given in Appendix S2.

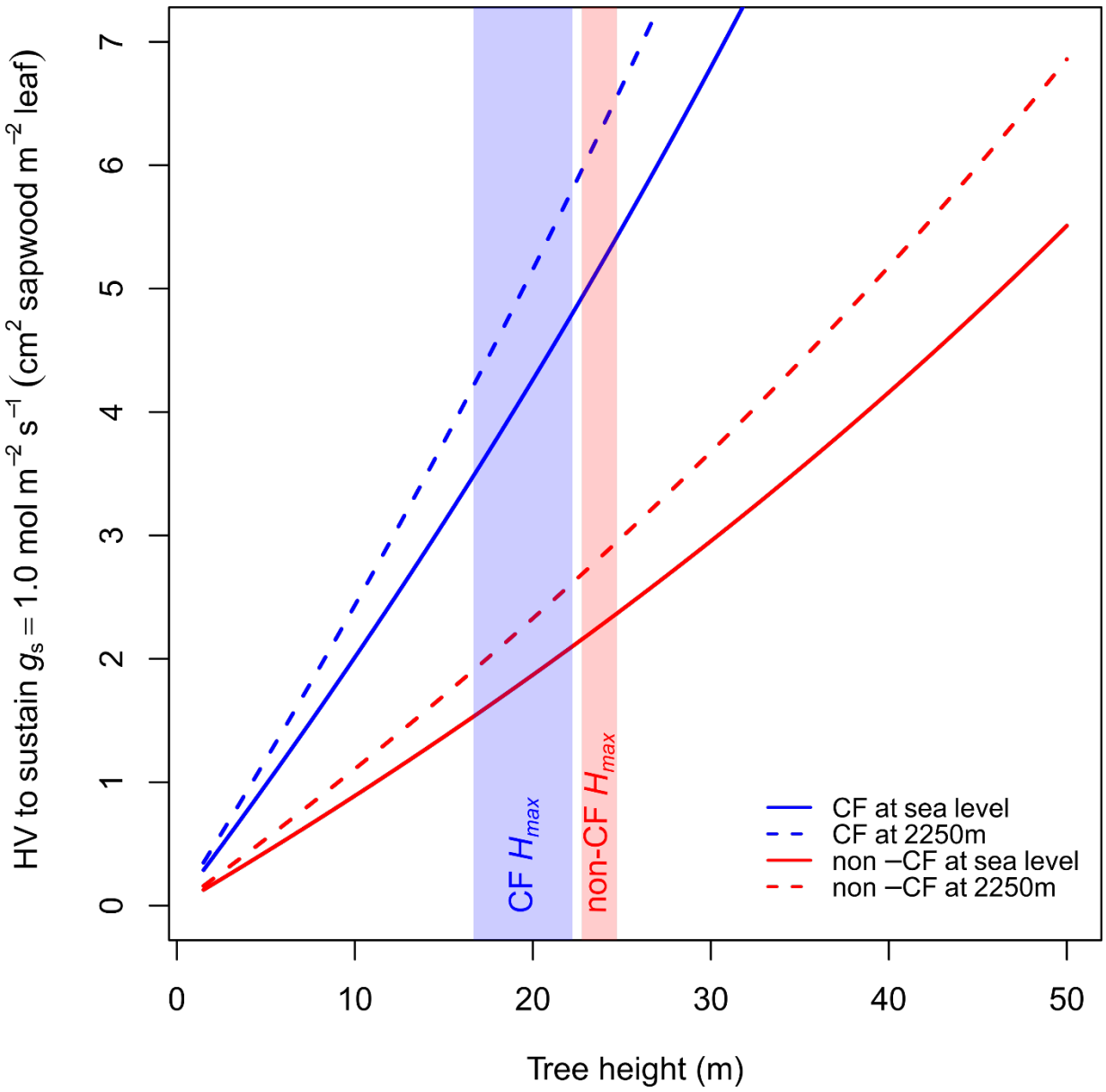

Figure 3. Huber Value (HV) necessary to sustain a stomatal conductance of 1 mol m^{-2} s^{-1} plotted in function of tree height. The blue lines represent Cloud Forests (CF) trees, and the blue lines represent non-CF trees. The dashed lines represent the environmental conditions at 2250 m. The differences in temperature between seal level and 2250 were based on the lapse rate from Fig. 2, and altitudinal changes in the incident shortwave radiation were modelled following Leuschner [42]. The red and blue shaded regions in the plot are the 95% confidence intervals of the mean tree height observed in CF and non-CF, respectively.

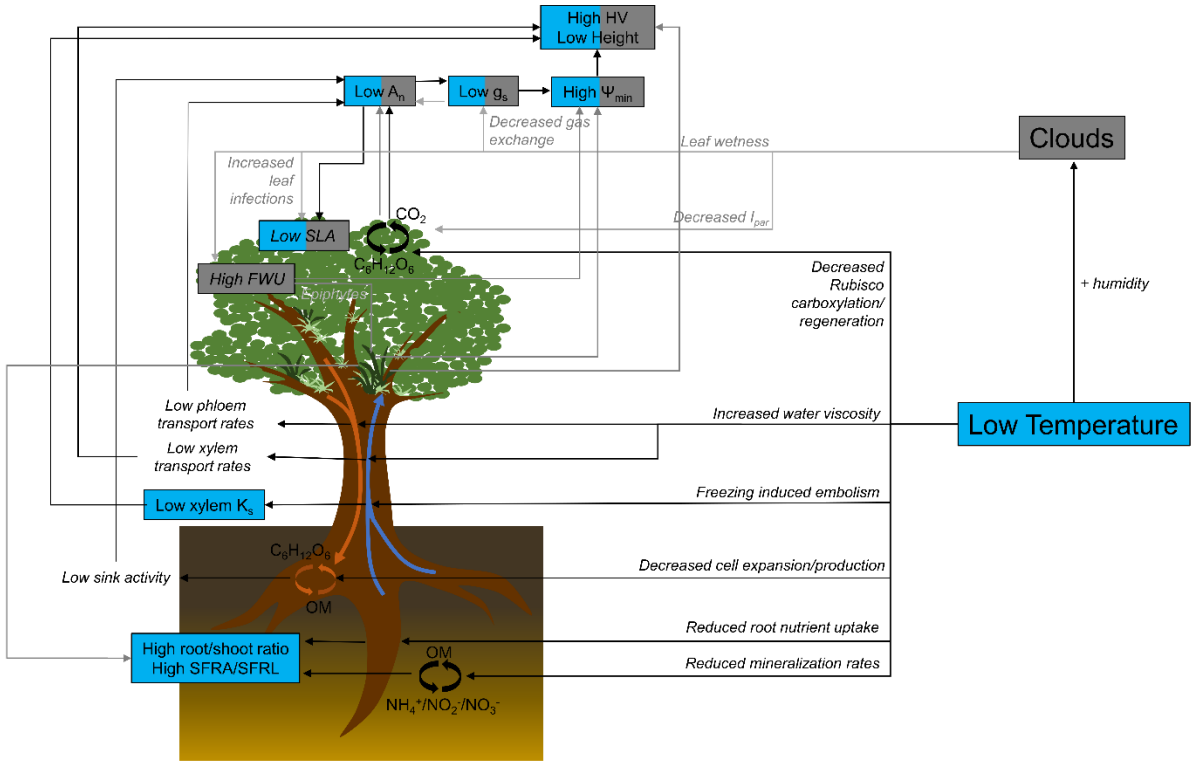

Figure 4. Schematic representation of the relationships between low temperatures and clouds on the Cloud Forest (CF) defining functional traits. The functional traits in blue boxes can be linked to low temperatures, while traits in gray boxes can be linked to clouds.